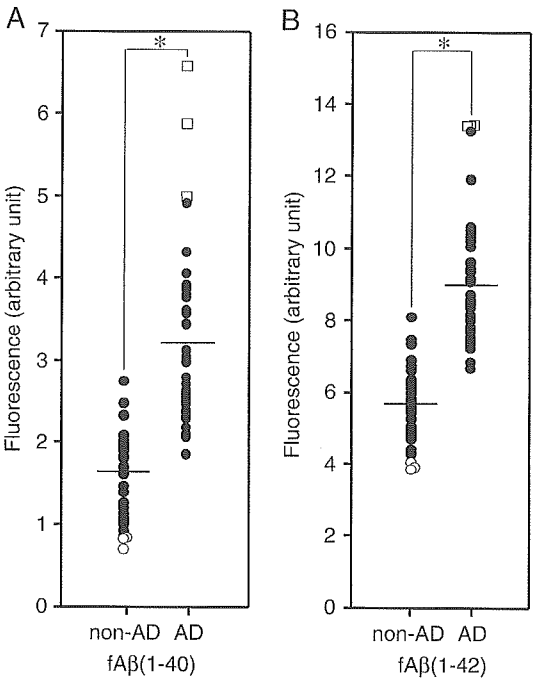

Fig. 2. Scatter plots of the final levels of fAβ(1–40) (A) and fAβ(1–42) formation (B) incubated with non-AD- or AD-CSF. ThT fluorescence 9 days (A) or 24 h (B) after the initiation of the reaction was plotted for non-AD (n = 40) and AD (n = 40) patients. The CSF obtained from 3 non-AD (○) and 3 AD patients (□) was further analyzed by electron microscopy (see Fig. 3). Each bar represents the mean value of each group. *P < 0.001, unpaired t test with Welch's correction.

and small amorphous aggregates were occasionally observed after incubation of fresh Aβ(1–40) with the CSF obtained from a non-AD patient (Figs. 2 and 3C). Similar morphology was observed after the incubation with the CSF obtained from 2 other AD patients and 2 other non-AD patients. We also obtained morphological findings after incubation of Aβ(1–42) with AD- and non-AD-CSF similar to those of Aβ(1–40) (data not shown). The control CSF samples without Aβs contained fine granules, round to polygonal particles with a diameter ranging from 20 to 80 nm, as well as occasional large aggregates with a diameter ranging from 100 to 250 nm (Fig. 3D). Similar morphology was observed with AD- and non-AD-CSF. Both fAβ(1–40) and fAβ(1–42) formed by incubation with non-AD-CSF were stained with Congo red to a lesser degree than those formed by incubation with AD-CSF (data not shown). These data may indicate that ThT assay reliably measures the formation of mature amyloid fibrils in our experimental conditions. However, we cannot rule out the possibility that Aβ oligomers, protofibrils, and other forms of Aβ aggregates are formed in the reaction mixture and ThT assay also detects them significantly.

Multiple comparisons between the final levels of fAβ formation after incubation with AD-CSF, and the levels of Aβ(1–42), tau, total protein, or IgG in CSF

In multiple comparisons between the final levels of fAβ(1–40) and fAβ(1–42) formation after incubation with AD–CSF, and the concentrations of Aβ(1–42), tau, total protein, IgG in CSF, only the levels of Aβ(1–42) were speculated to influence the final

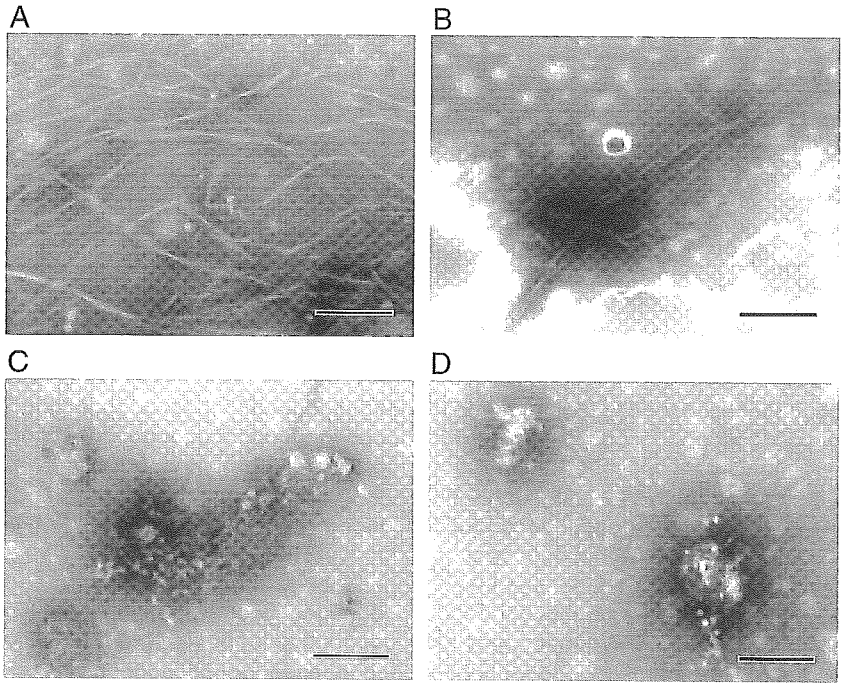

Fig. 3. Electron micrographs of fAβ(1–40) formed with or without CSF and the control CSF sample without Aβs. The reaction mixtures containing 50 μM Aβ(1–40), 50 mM phosphate buffer, pH 7.5, 100 mM NaCl, and 0 (A) or 78% (vol/vol) CSF obtained from an AD (B) or a non-AD patient (C) were incubated at 37°C for 9 days. Similar morphology was observed with the CSF of 2 other AD and 2 other non-AD patients (data not shown). See the legend to Fig. 2. The control mixture containing 50 mM phosphate buffer, pH 7.5, 100 mM NaCl, and 78% (vol/vol) CSF obtained from an AD patient (D) was also examined. Similar morphology was observed with the CSF of 2 other AD and 3 other non-AD patients (data not shown). Scale bars indicate a length of 250 nm.

levels of fAβs formation [$F = 11.729$, $P < 0.01$ in fAβ(1–40) formation, $F = 4.751$, $P < 0.05$ in fAβ(1–42) formation].

Correlation between the final level of fAβ formation after incubation with AD-CSF and the concentrations of Aβ(1–42) in CSF

As shown in Figs. 4A and B, the final levels of fAβ(1–40) and fAβ(1–42) formation after incubation with AD–CSF showed a significant negative correlation with the concentration of Aβ(1–42) in CSF ($r = 0.486$, $P < 0.01$ in Fig. 4A; $r = 0.333$, $P < 0.05$ in Fig. 4B).

Correlation between the final level of fAβ formation after incubation with AD-CSF, and MMSE score, clinical course, and apoE phenotype of AD patients

The final levels of fAβ(1–40) and fAβ(1–42) formation after incubation with AD-CSF were not significantly correlated with MMSE score and clinical course (data not shown). The final levels of fAβ(1–40) and fAβ(1–42) formation after incubation with AD-CSF were not significantly correlated with the number (i.e., 0, 1, or 2) of E4 isoform of apoE (data not shown).

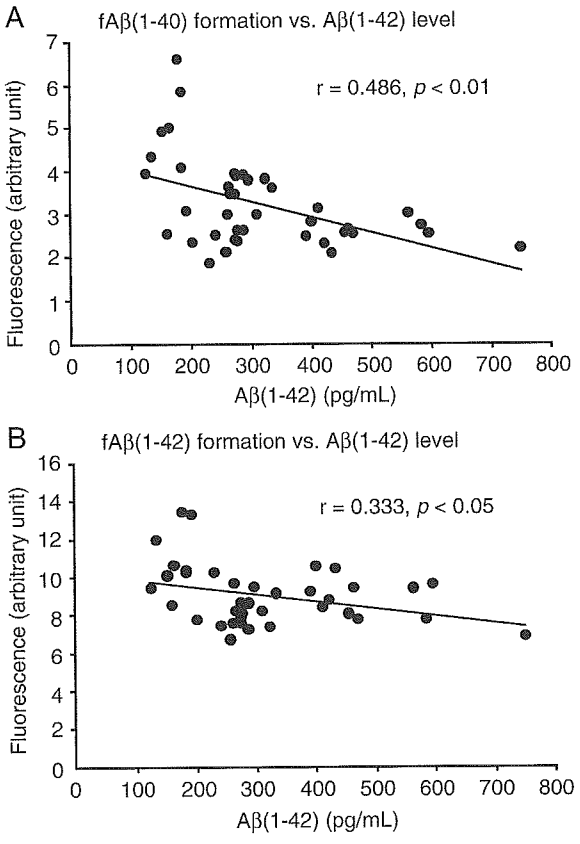

Fig. 4. Correlation of the final levels of fAβ(1–40) (A) and fAβ(1–42) formation (B) incubated with AD-CSF, with the concentration of Aβ(1–42) in CSF. ThT fluorescence 9 days (A) or 24 h (B) after the initiation of the reaction was plotted against the concentration of Aβ(1–42) in CSF. In both cases, significant negative correlations were observed between the final levels and Aβ(1–42) concentration ($r = 0.486$, $P < 0.01$ in panel A, $r = 0.333$, $P < 0.05$ in panel B, Pearson's correlation test).

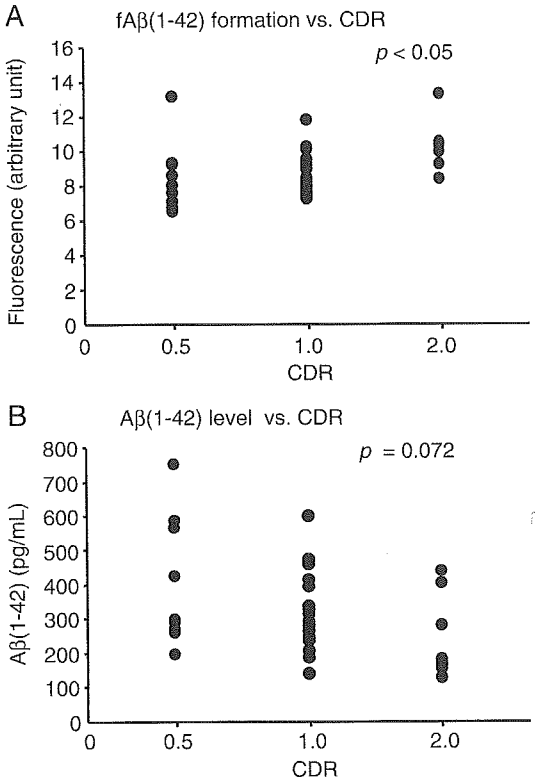

Fig. 5. Associations of the final level of fAβ(1–42) formation after incubation with AD-CSF (A) and the concentration of Aβ(1–42) in AD-CSF (B), with CDR. ThT fluorescence 24 h after the initiation of the reaction (A) and Aβ(1–42) concentration (B) are plotted against CDR. In panel A, a significant association is observed between the final level of fAβ(1–42) formation and CDR ($P < 0.05$, Kruskal-Wallis test). In panel B, the concentration of Aβ(1–42) in AD-CSF was lower with increasing CDR, but this association was not significant ($P = 0.072$, Kruskal-Wallis test).

Association between the final level of fAβ formation after incubation with AD-CSF, and CDR of AD patients

Although the final level of fAβ(1–40) formation after incubation with AD-CSF was not significantly associated with CDR (data not shown), the final level of fAβ(1–42) formation after incubation with AD-CSF was significantly associated with CDR ($P < 0.05$) (Fig. 5A). The concentration of Aβ(1–42) in AD-CSF was lower with increasing CDR, but this association was not significant ($P = 0.072$) (Fig. 5B).

Discussion

Both AD-CSF and non-AD-CSF inhibited the formation of fAβ(1–40) and fAβ(1–42). Moreover, non-AD-CSF ($n = 40$) inhibited the formation of fAβs significantly more strongly than AD-CSF ($n = 40$). Although Wisniewski et al. (1993) reported previously that fAβ(1–40) formation is inhibited by CSF using ThT fluorometry and electron microscopy, they found no significant difference in the inhibitory effect between AD-CSF and control CSF. They examined the effect of the CSF obtained from 5 normal patients and 5 AD patients and followed the ThT kinetics at 10, 20, and 70 h after the initiation of the reaction. The

small number of cases examined and the preliminary kinetic analysis may be the reasons why they observed no significant difference between AD and control groups. The limitation of our study is that only non-AD patients with other neurologic disorders served as a control group, requiring further study with CSF samples from healthy individuals to confirm our results.

The weaker inhibitory activity of AD-CSF may be due to the decrease in the specific inhibitors of fAβ formation in the CSF of AD patients. After Wisniewski et al. (1993) suggested that CSF contains one or more inhibitors of fibril formation, various groups reported that some inhibitors of fAβ formation in vitro, such as apoE, TTR, and anti-Aβ antibodies, are significantly reduced in the CSF of AD patients as compared to age-matched controls (Blennow et al., 1994; Du et al., 2001; Kunicki et al., 1998; Serot et al., 1997). We and other groups suggested that apoE, apoJ, TTR, α2M, and anti-Aβ antibodies inhibit fAβ formation by making a complex with Aβ, thus eliminating free Aβ from the reaction mixture (Calero et al., 2000; Du et al., 1998, 2003; Naiki et al., 1998; Schwarzman et al., 1994). Similarly, Eriksson et al. (1995) also suggested that the influence of ACT on fAβ formation may be an example of hydrophobic interaction between Aβ and the hydrophobic domain C terminal to the reactive center of ACT. Although Janciauskiene et al. (1995) suggested that SAP impedes the seeding process and inhibits the fibril growth by binding to Aβ and preventing Aβ–Aβ polymerization, Kimura et al. (1999) found no significant difference in the SAP level in CSF between AD and control groups. In our study, the final levels of fAβs after incubation with AD-CSF was not significantly correlated with the concentrations of total protein and IgG in AD-CSF, as well as with apoE phenotype of AD patients. However, as apoE phenotyping was limited to 34 of 40 AD patients in our study, further analysis with a larger number of samples is essential for more exact correlation. A particular set of the above-described molecules may additively or synergistically contribute to inhibit fAβ formation in vitro.

Another possibility is that the specific factors accelerating fAβ formation may be increased in the CSF of AD patients. Ma et al. (1994) suggested that apoE and ACT each recognizes and binds to Aβ to promote filament formation but at different sites and with different degrees of specificity. In some clinical situations, apoE and ACT may also act as a promoter of fAβ formation. Recently, Pitschke et al. (1998) reported a biophysical method that used the principle of seeded polymerization in combination with fluorescence correlation spectroscopy, which allowed them to detect single Aβ aggregates in the CSF samples from AD patients. All 15 AD samples but none of the 19 age-matched control samples produced large peaks with fluorescence correlation spectroscopy indicating the rapid aggregation of the fluorescent labeled synthetic Aβ probe onto the Aβ seeds present in the CSF. The importance of such early aggregates or oligomers for fAβ formation and neurotoxicity has been reported by some other investigators (Bucciantini et al., 2002; Hartley et al., 1999; Kayed et al., 2003; Podlisny et al., 1995; Walsh et al., 1997, 1999; Xia et al., 1997). The net inhibitory potential of CSF for fAβ formation in vitro may be determined by the total balance between the above-described inhibitors and accelerators in CSF. In order to understand the nature of this molecular balance, it may be essential to determine systematically the concentrations of the specific inhibitors and accelerators in AD- and non-AD-CSF.

The final levels of fAβ(1–40) and fAβ(1–42) formation after incubation with AD-CSF showed a significant negative correlation with the concentration of Aβ(1–42) in CSF (Figs. 4A and B). The final level of fAβ(1–42) formation after incubation with AD-CSF also showed a significant association with CDR (Fig. 5A). Moreover, although an association between the concentration of Aβ(1–42) in AD-CSF and CDR was not significant, the concentration of Aβ(1–42) had a tendency to be lower with increasing CDR (Fig. 5B), indicating that Aβ(1–42) level in CSF decreases according to the progression of AD. Jensen et al. (1999) also reported that the Aβ(1–42) level in AD-CSF declines with the progression of AD. Overall, our correlation analysis indicates that the final levels of fAβ(1–40) and fAβ(1–42) formation after incubation with AD-CSF increase in parallel with the progression of AD. Recently, Strozyk et al. (2003) suggested that lower Aβ(1–42) levels reflect a neuropathologic process implicated in amyloid-related pathologies, such as neuritic plaques and cerebral amyloid angiopathy in a population-based autopsy study. In parallel with the amyloid-related consumption of Aβ(1–42) in CSF, the specific inhibitors of fAβ formation in CSF may also be trapped in the Aβ-related pathologies. Such a decrease in the concentration of the inhibitors in CSF may increase the final level of fAβ formation after incubation with AD-CSF. Alternatively, the specific factors accelerating fAβ formation may be increased in parallel with the progression of AD. This may also contribute to the increase in the final level of fAβ formation.

In conclusion, our study indicates that AD-CSF is a favorable molecular environment for the Aβ-related pathologies than non-AD-CSF, and the environment may become more favorable for the Aβ-related pathologies with the progression of AD. These interpretations further support the Aβ cascade hypothesis of AD (Du et al., 2003). To determine the inhibitors and accelerators for fAβ formation in CSF, further investigation is necessary including the association studies between the degree of fAβ formation and concentrations of candidate molecules which are known or newly identified by a proteome analysis of AD- and non-AD-CSF.

Acknowledgments

This work was supported in part by a Grant-in-Aid for Scientific Research (M.Y.), a grant for the 21st Century COE Program (on Innovative Brain Science for Development, Learning, and Memory) (M.Y.), a grant for the Knowledge Cluster Initiative [High-Tech Sensing and Knowledge Handling Technology (Brain Technology)] (M.Y.), and a Grant-in-Aid for Scientific Research on Priority Areas (C) -Advanced Brain Science Project (H.N.) from the Ministry of Education, Culture, Sports, Science and Technology, Japan, and a grant to the Amyloidosis Research Committee from the Ministry of Health, Labor, and Welfare, Japan (M.Y.).

The authors thank Drs. M. Samuraki, M. Hirohata, Y. Furukawa, T. Hamaguchi, M. Yoshita, S. Okino, and K. Komai (Kanazawa University) for cooperation in the experiments, Dr. I. Kuji (Kanazawa University) for the data analysis, and Y. Kakuda, Y. Yamaguchi (Kanazawa University), H. Okada, and N. Takimoto (University of Fukui) for excellent technical assistance.

References

Andreasen, N., Hesse, C., Davidsson, P., Minthon, L., Wallin, A., Winblad, B., Vanderstichele, H., Vanmechelen, E., Blennow, K., 1999. Cerebrospinal fluid beta-amyloid(1–42) in Alzheimer disease: differences between early- and late-onset Alzheimer discase and stability during the course of disease. Arch. Neurol. 56, 673–680.

Beyreuther, K., Masters, C.L., 1997. Alzheimer's disease. The ins and outs of amyloid-beta. Nature 389, 677–678.

Blennow, K., Hesse, C., Fredman, P., 1994. Cerebrospinal fluid apolipoprotein E is reduced in Alzheimer's disease. NeuroReport 5, 2534–2536.

Blennow, K., Wallin, A., Agren, H., Spenger, C., Siegfried, J., Vanmechelen, E., 1995. Tau protein in cerebrospinal fluid: a biochemical marker for axonal degeneration in Alzheimer disease? Mol. Chem. Neuropathol. 26, 231–245.

Bucciantini, M., Giannoni, E., Chiti, F., Baroni, F., Formigli, L., Zurdo, J., Taddei, N., Ramponi, G., Dobson, C.M., Stefani, M., 2002. Inherent toxicity of aggregates implies a common mechanism for protein misfolding diseases. Nature 416, 507–511.

Calero, M., Rostagno, A., Matsubara, E., Zlokovic, B., Frangione, B., Ghiso, J., 2000. Apolipoprotein J (clusterin) and Alzheimer's disease. Microsc. Res. Tech. 50, 305–315.

Du, Y., Bales, K.R., Dodel, R.C., Liu, X., Glinn, M.A., Horn, J.W., Little, S.P., Paul, S.M., 1998. Alpha2-macroglobulin attenuates beta-amyloid peptide 1–40 fibril formation and associated neurotoxicity of cultured fetal rat cortical neurons. J. Neurochem. 70, 1182–1188.

Du, Y., Dodel, R., Hampel, H., Buerger, K., Lin, S., Eastwood, B., Bales, K., Gao, F., Moeller, H.J., Oertel, W., Farlow, M., Paul, S., 2001. Reduced levels of amyloid beta-peptide antibody in Alzheimer disease. Neurology 57, 801–805.

Du, Y., Wei, X., Dodel, R., Sommer, N., Hampel, H., Gao, F., Ma, Z., Zhao, L., Oertel, W.H., Farlow, M., 2003. Human anti-beta-amyloid antibodies block beta-amyloid fibril formation and prevent beta-amyloid-induced neurotoxicity. Brain 126, 1935–1939.

Eriksson, S., Janciauskiene, S., Lannfelt, L., 1995. Alpha 1-antichymotrypsin regulates Alzheimer beta-amyloid peptide fibril formation. Proc. Natl. Acad. Sci. U. S. A. 92, 2313–2317.

Esler, W.P., Stimson, E.R., Ghilardi, J.R., Vinters, H.V., Lee, J.P., Mantyh, P.W., Maggio, J.E., 1996. In vitro growth of Alzheimer's disease beta-amyloid plaques displays first-order kinetics. Biochemistry 35, 749–757.

Ewbank, D.C., 1999. Deaths attributable to Alzheimer's disease in the United States. Am. J. Public Health 89, 90–92.

Folstein, M.F., Folstein, S.E., McHugh, P.R., 1975. "Mini-mental state". A practical method for grading the cognitive state of patients for the clinician. J. Psychiatr. Res. 12, 189–198.

Fritz, R.B., Rivers, S.L., 1972. Hepatitis-associated antigen: detection by antibody-sensitized latex particles. J. Immunol. 108, 108–111.

Fujita, Y., Mori, I., Kitano, S., 1984. Determination of proteins by using the color reaction with pyrocatechol violet–molybdenum(VI) complex. Chem. Pharm. Bull. (Tokyo) 32, 4161–4164.

Haass, C., Schlossmacher, M.G., Hung, A.Y., Vigo-Pelfrey, C., Mellon, A., Ostaszewski, B.L., Lieberburg, I., Koo, E.H., Schenk, D., Teplow, D.B., Selkoe, D.J., 1992. Amyloid beta-peptide is produced by cultured cells during normal metabolism. Nature 359, 322–325.

Harper, J.D., Wong, S.S., Lieber, C.M., Lansbury Jr., P.T., 1999. Assembly of A beta amyloid protofibrils: an in vitro model for a possible early event in Alzheimer's disease. Biochemistry 38, 8972–8980.

Hartley, D.M., Walsh, D.M., Ye, C.P., Diehl, T., Vasquez, S., Vassilev, P.M., Teplow, D.B., Selkoe, D.J., 1999. Protofibrillar intermediates of amyloid beta-protein induce acute electrophysiological changes and progressive neurotoxicity in cortical neurons. J. Neurosci. 19, 8876–8884.

Hasegawa, K., Yamaguchi, I., Omata, S., Gejyo, F., Naiki, H., 1999. Interaction between A beta(1–42) and A beta(1–40) in Alzheimer's beta-amyloid fibril formation in vitro. Biochemistry 38, 15514–15521.

Hughes, C.P., Berg, L., Danziger, W.L., Coben, L.A., Martin, R.L., 1982. A new clinical scale for the staging of dementia. Br. J. Psychiatry 140, 566–572.

Janciauskiene, S., Garcia de Fruntos, P., Carlemalm, E., Dahlback, B., Eriksson, S., 1995. Inhibition of Alzheimer beta-peptide fibril formation by serum amyloid P component. J. Biol. Chem. 270, 26041–26044.

Jarrett, J.T., Lansbury Jr., P.T., 1993. Seeding "one-dimensional crystallization" of amyloid: a pathogenic mechanism in Alzheimer's disease and scrapie? Cell 73, 1055–1058.

Jensen, M., Schroder, J., Blomberg, M., Engvall, B., Pantel, J., Ida, N., Basun, H., Wahlund, L.O., Werle, E., Jauss, M., Beyreuther, K., Lannfelt, L., Hartmann, T., 1999. Cerebrospinal fluid A beta42 is increased early in sporadic Alzheimer's disease and declines with disease progression. Ann. Neurol. 45, 504–511.

Kang, J., Lemaire, H.G., Unterbeck, A., Salbaum, J.M., Masters, C.L., Grzeschik, K.H., Multhaup, G., Beyreuther, K., Muller-Hill, B., 1987. The precursor of Alzheimer's disease amyloid A4 protein resembles a cell-surface receptor. Nature 325, 733–736.

Kataoka, S., Paidi, M., Howard, B.V., 1994. Simplified isoelectric focusing/immunoblotting determination of apoprotein E phenotype. Clin. Chem. 40, 11–13.

Kayed, R., Head, E., Thompson, J.L., McIntire, T.M., Milton, S.C., Cotman, C.W., Glabe, C.G., 2003. Common structure of soluble amyloid oligomers implies common mechanism of pathogenesis. Science 300, 486–489.

Kimura, M., Asada, T., Uno, M., Machida, N., Kasuya, K., Taniguchi, Y., Fujita, T., Nishiyama, E., Iwamoto, N., Arai, H., 1999. Assessment of cerebrospinal fluid level of serum amyloid P component in patients with Alzheimer's disease. Neurosci. Lett. 273, 137–139.

Kunicki, S., Richardson, J., Mehta, P.D., Kim, K.S., Zorychta, E., 1998. The effects of age, apolipoprotein E phenotype and gender on the concentration of amyloid-beta (A beta) 40, A beta 42, apolipoprotein E and transthyretin in human cerebrospinal fluid. Clin. Biochem. 31, 409–415.

Lomakin, A., Teplow, D.B., Kirschner, D.A., Benedek, G.B., 1997. Kinetic theory of fibrillogenesis of amyloid beta-protein. Proc. Natl. Acad. Sci. U. S. A. 94, 7942–7947.

Ma, J., Yee, A., Brewer Jr., H.B., Das, S., Potter, H., 1994. Amyloid-associated proteins alpha 1-antichymotrypsin and apolipoprotein E promote assembly of Alzheimer beta-protein into filaments. Nature 372, 92–94.

McKhann, G., Drachman, D., Folstein, M., Katzman, R., Price, D., Stadlan, E.M., 1984. Clinical diagnosis of Alzheimer's disease: report of the NINCDS-ADRDA Work Group under the auspices of Department of Health and Human Services Task Force on Alzheimer's Disease. Neurology 34, 939–944.

Naiki, H., Gejyo, F., 1999. Kinetic analysis of amyloid fibril formation. Methods Enzymol. 309, 305–318.

Naiki, H., Nakakuki, K., 1996. First-order kinetic model of Alzheimer's beta-amyloid fibril extension in vitro. Lab. Invest. 74, 374–383.

Naiki, H., Gejyo, F., Nakakuki, K., 1997. Concentration-dependent inhibitory effects of apolipoprotein E on Alzheimer's beta-amyloid fibril formation in vitro. Biochemistry 36, 6243–6250.

Naiki, H., Hasegawa, K., Yamaguchi, I., Nakamura, H., Gejyo, F., Nakakuki, K., 1998. Apolipoprotein E and antioxidants have different mechanisms of inhibiting Alzheimer's beta-amyloid fibril formation in vitro. Biochemistry 37, 17882–17889.

Pitschke, M., Prior, R., Haupt, M., Riesner, D., 1998. Detection of single amyloid beta-protein aggregates in the cerebrospinal fluid of Alzheimer's patients by fluorescence correlation spectroscopy. Nat. Med. 4, 832–834.

Podlisny, M.B., Ostaszewski, B.L., Squazzo, S.L., Koo, E.H., Rydell, R.E., Teplow, D.B., Selkoe, D.J., 1995. Aggregation of secreted amyloid beta-protein into sodium dodecyl sulfate-stable oligomers in cell culture. J. Biol. Chem. 270, 9564–9570.

Schmechel, D.E., Saunders, A.M., Strittmatter, W.J., Crain, B.J., Hulette, C.M., Joo, S.H., Pericak-Vance, M.A., Goldgaber, D., Roses, A.D.,

1993. Increased amyloid beta-peptide deposition in cerebral cortex as a consequence of apolipoprotein E genotype in late-onset Alzheimer disease. Proc. Natl. Acad. Sci. U. S. A. 90, 9649–9653.

Schwarzman, A.L., Gregori, L., Vitek, M.P., Lyubski, S., Strittmatter, W.J., Enghilde, J.J., Bhasin, R., Silverman, J., Weisgraber, K.H., Coyle, P.K., Zagorski, M.G., Talafous, J., Eisenberg, M., Saunders, A.M., Roses, A.D., Goldgaber, D., 1994. Transthyretin sequesters amyloid beta protein and prevents amyloid formation. Proc. Natl. Acad. Sci. U. S. A. 91, 8368–8372.

Selkoe, D.J., 2001. Alzheimer's disease: genes, proteins, and therapy. Physiol. Rev. 81, 741–766.

Serot, J.M., Christmann, D., Dubost, T., Couturier, M., 1997. Cerebrospinal fluid transthyretin: aging and late onset Alzheimer's disease. J. Neurol., Neurosurg. Psychiatry 63, 506–508.

Strozyk, D., Blennow, K., White, L.R., Launer, L.J., 2003. CSF Abeta 42 levels correlate with amyloid-neuropathology in a population-based autopsy study. Neurology 60, 652–656.

Vandermeeren, M., Mercken, M., Vanmechelen, E., Six, J., Van De Voorde, A., Martin, J.J., Cras, P., 1993. Detection of tau proteins in normal and Alzheimer's disease cerebrospinal fluid with a sensitive sandwich enzyme-linked immunosorbent assay. J. Neurochem. 61, 1828–1834.

Vanderstichele, H., Blennow, K., D'Heuvaert, N., Buyse, M-A., Wallin, A., Andreasen, N., Seubert, P., Van De Voorde, A., Vanmechelen, E., 1998. Development of a specific diagnostic test for the measurement of β-amyloid(1–42) in CSF. In: Fisher, A., Hanin, I., Yoshida, M., (Eds.), Progress in Alzheimer's and Parkinson's Diseases. Plenum Publishing Corp, New York, pp. 773–778.

Walsh, D.M., Lomakin, A., Benedek, G.B., Condron, M.M., Teplow, D.B., 1997. Amyloid beta-protein fibrillogenesis. Detection of a protofibrillar intermediate. J. Biol. Chem. 272, 22364–22372.

Walsh, D.M., Hartley, D.M., Kusumoto, Y., Fezoui, Y., Condron, M.M., Lomakin, A., Benedek, G.B., Selkoe, D.J., Teplow, D.B., 1999. Amyloid beta-protein fibrillogenesis. Structure and biological activity of protofibrillar intermediates. J. Biol. Chem. 274, 25945–25952.

Wisniewski, T., Castano, E., Ghiso, J., Frangione, B., 1993. Cerebrospinal fluid inhibits Alzheimer beta-amyloid fibril formation in vitro. Ann. Neurol. 34, 631–633.

Xia, W., Zhang, J., Kholodenko, D., Citron, M., Podlisny, M.B., Teplow, D.B., Haass, C., Seubert, P., Koo, E.H., Selkoe, D.J., 1997. Enhanced production and oligomerization of the 42-residue amyloid beta-protein by Chinese hamster ovary cells stably expressing mutant presenilins. J. Biol. Chem. 272, 7977–7982.

Available online at www.sciencedirect.com
SCIENCE DIRECT®
ELSEVIER
Biochemical and Biophysical Research Communications 330 (2005) 111–116
BBRC
www.elsevier.com/locate/ybbrc

Preformed β-amyloid fibrils are destabilized by coenzyme Q_{10} in vitro

Kenjiro Ono [a], Kazuhiro Hasegawa [b], Hironobu Naiki [b], Masahito Yamada [a,*]

[a] *Department of Neurology and Neurobiology of Aging, Kanazawa University Graduate School of Medical Science, Kanazawa 920-8640, Japan*
[b] *Department of Pathology, Fukui University, Fukui 910-1193, CREST of Japan Science and Technology Corporation, Kawaguchi 332-0012, Japan*

Received 2 February 2005

Abstract

Inhibition of the formation of β-amyloid fibrils (fAβ), as well as the destabilization of preformed fAβ in the CNS, would be attractive therapeutic targets for the treatment of Alzheimer's disease (AD). We reported previously that nordihydroguaiaretic acid (NDGA) and wine-related polyphenol, myricetin (Myr), inhibit fAβ formation from Aβ and destabilize preformed fAβ in vitro. Using fluorescence spectroscopic analysis with thioflavin T and electron microscopic studies, we examined the effects of coenzyme Q_{10} (CoQ_{10}) on the formation, extension, and destabilization of fAβ at pH 7.5 at 37 °C in vitro. We next compared the anti-amyloidogenic activities of CoQ_{10} with NDGA and Myr. CoQ_{10} dose-dependently inhibited fAβ formation from amyloid β-peptide (Aβ), as well as their extension. Moreover, it destabilized preformed fAβs. The anti-amyloidogenic effects of CoQ_{10} were slightly weaker than those of NDGA and Myr. CoQ_{10} could be a key molecule for the development of therapeutics for AD.

Keywords: Alzheimer's disease; Coenzyme Q_{10}; β-Amyloid fibrils; Thioflavin T; Electron microscopy

Alzheimer's disease (AD) is the most common cause of dementia in aged humans, affecting ~200 million people worldwide [1]. The disease is characterized by extracellular deposition of amyloid β-peptide (Aβ) in senile plaques, intracellular appearance of neurofibrillary tangles, and synaptic and neuronal loss [2]. Considerable effort is currently directed toward the development of anti-amyloid therapeutics as possible strategies to prevent or treat AD. Using a nucleation-dependent polymerization model to explain the mechanism of the formation of Alzheimer's β-amyloid fibrils (fAβ) in vitro [3,4], we previously found that nordihydroguaiaretic acid (NDGA) and rifampicin (RIF) inhibit fAβ formation dose-dependently in vitro [5]. Moreover, we reported that they also destabilize fAβ(1–40) and fAβ(1–42) in a concentration-dependent manner, based on fluorescence spectroscopic analysis with thioflavin T (ThT) and electron microscopic studies [6].

A large number of studies indicate that oxidative injury may play a role in the development of AD [7]. Many antioxidant compounds, such as vitamin E [8], NDGA [9], and nicotine [10], have been demonstrated to protect the brain from in vitro Aβ toxicity. Recently, we showed that the wine-related polyphenols such as myricetin (Myr), and the lipophilic antioxidant, vitamin A, dose-dependently inhibit formation and extension of fAβ(1–40) and fAβ(1–42), as well as destabilizing preformed fAβs in vitro [11,12]. As similar to vitamin A, coenzyme Q_{10} (CoQ_{10}) is well known to be an important lipid-soluble antioxidant [13]. Soderberg et al. [14] found increased levels of CoQ_{10} in most regions of the brains of patients with AD. A recent study by Bustos et al. [15] found no significant difference in plasma CoQ_{10} levels between patients with AD and controls. Although Imagawa et al. [16] reported a marked improvement in mental state of two sisters with genetically confirmed AD after a combined therapy with CoQ_{10}, iron, and vitamin B6, no large clinical studies assessing the cognitive effect of oral supplementation of CoQ_{10} in AD have

* Corresponding author. Fax: +81 76 234 4253.
E-mail address: m-yamada@med.kanazawa-u.ac.jp (M. Yamada).

0006-291X/$ - see front matter © 2005 Elsevier Inc. All rights reserved.
doi:10.1016/j.bbrc.2005.02.132

been performed. Here, we examined the effects of CoQ_{10} to inhibit the formation, extension of fAβ(1–40) and fAβ(1–42), as well as to destabilize fAβs at pH 7.5 at 37 °C in vitro, using fluorescence spectroscopy with ThT and electron microscopy. We also compared its anti-amyloidogenic and fibril-destabilizing effects with those of NDGA and Myr.

Materials and methods

Preparation of Aβ and fAβ solutions. Aβ(1–40) (a trifluoroacetate salt, Peptide Institute, Osaka, Japan) and Aβ(1–42) (a trifluoroacetate salt, Peptide Institute) were dissolved by brief vortexing in a 0.02% ammonia solution at a concentration of 500 μM (2.2 mg/mL) and 250 μM, respectively, in a 4 °C room and stored at −80 °C before assaying (fresh Aβ(1–40) and Aβ(1–42) solutions). fAβ(1–40) and fAβ(1–42) were formed from the fresh Aβ(1–40) and Aβ(1–42) solutions, respectively, sonicated, and stored at 4 °C as described elsewhere [17].

Fresh, non-aggregated fAβ(1–40) and fAβ(1–42) were obtained by extending sonicated fAβ(1–40) or fAβ(1–42) with fresh Aβ(1–40) or Aβ(1–42) solutions, respectively, just before the destabilization reaction [6,11,12,18]. The reaction mixture was 600 μL and contained 10 μg/mL fAβ(1–40) or fAβ(1–42), 50 μM Aβ(1–40) or Aβ(1–42), 50 mM phosphate buffer, pH 7.5, and 100 mM NaCl. Measurement of the fluorescence of ThT showed that the extension reaction proceeded to equilibrium after incubation at 37 °C for 3–6 h under non-agitated conditions. In the following experiment, the concentration of fAβ(1–40) and fAβ(1–42) in the final reaction mixture was regarded as 50 μM.

Fluorescence spectroscopy, electron microscopy, and polarized light microscopy. A fluorescence spectroscopic study was performed on a Hitachi F-2500 fluorescence spectrophotometer as described elsewhere [19]. Optimum fluorescence measurements of fAβ(1–40) and fAβ(1–42) were obtained at the excitation and emission wavelengths of 445 and 490 nm, respectively, with the reaction mixture containing 5 μM ThT (Wako Pure Chemical Industries, Osaka, Japan) and 50 mM glycine–NaOH buffer, pH 8.5. Electron microscopic and polarized light microscopic studies of the reaction mixtures were performed as described elsewhere [17].

Polymerization assay. Polymerization of Aβ with or without fAβ added as seeds was assayed as described elsewhere [5]. Briefly, the reaction mixture contained 50 μM Aβ(1–40), or 25 or 50 μM Aβ(1–42), 0 or 10 μg/mL fAβ(1–40) or fAβ(1–42), 0–50 μM CoQ_{10}, NDGA, or Myr (Sigma Chemical, St. Louis, MO), 1% dimethyl sulfoxide (DMSO), 50 mM phosphate buffer, pH 7.5, and 100 mM NaCl.

Thirty-microliter aliquots of the mixture were put into oil-free PCR tubes (Takara Shuzo, Otsu, Japan). These tubes were then put into a DNA thermal cycler (PJ480, Perkin-Elmer Cetus, Emeryville, California). Starting at 4 °C, the plate temperature was elevated at maximal speed, to 37 °C. Incubation times ranged between 0 and 8 days as indicated in each figure. The tubes were not agitated during the reaction. Five microliter aliquots from each tube in triplicate were subjected to fluorescence spectroscopy and the mean of the three measurements was determined. In the ThT solution, the concentration of CoQ_{10}, NDGA, and Myr examined in this study was diluted up to

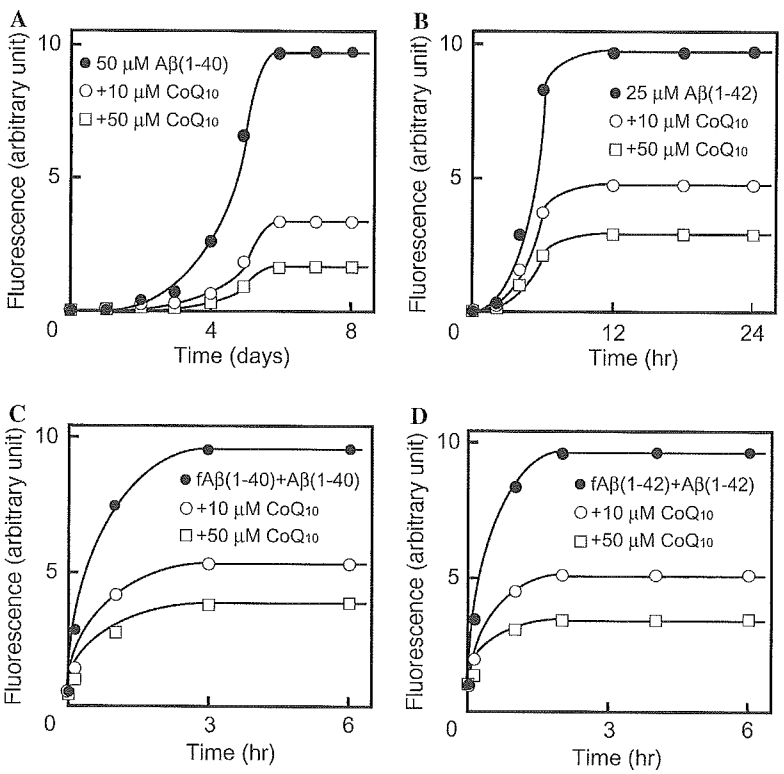

Fig. 1. CoQ_{10} inhibits the formation of fAβ. Effects of CoQ_{10} on the kinetics of formation of fAβ(1–40) (A) and fAβ(1–42) (B) from fresh Aβ(1–40) and Aβ(1–42), respectively. The reaction mixtures containing 50 μM Aβ(1–40) (A) or 25 μM Aβ(1–42) (B), 50 mM phosphate buffer, pH 7.5, 100 mM NaCl, and 0 (●), 10 (○), or 50 μM (□) of CoQ_{10} were incubated at 37 °C for the indicated times. Each figure shows a representative pattern of three independent experiments. (C,D) Effects of CoQ_{10} on the kinetics of fAβ(1–40) and fAβ(1–42) extension. The reaction mixtures containing 10 μg/mL sonicated fAβ(1–40) (C) or fAβ(1–42) (D), 50 μM Aβ(1–40) (C) or Aβ(1–42) (D), 50 mM phosphate buffer, pH 7.5, 100 mM NaCl, and 0 (●), 10 (○), or 50 μM (□) of CoQ_{10} were incubated at 37 °C for the indicated times. Each figure shows a representative pattern of three independent experiments.

1/200 of that in the reaction mixture. We confirmed that these compounds did not quench ThT fluorescence at the diluted concentration (data not shown).

Measurement of fibril-destabilizing activity. Destabilization of fAβ was assayed as described elsewhere [6]. Briefly, the reaction mixture contained 25 μM fresh fAβ(1–40) or fAβ(1–42), 0–50 μM CoQ_{10}, NDGA, or Myr, 1% DMSO, 50 mM phosphate buffer, pH 7.5, 100 mM NaCl, and 1%(wt/vol.) polyvinyl alcohol (Wako Pure Chemical Industries) to avoid the aggregation of fAβ and the adsorption of fAβ onto the inner wall of the reaction tube during the reaction.

After being mixed by pipetting, triplicate 5-μL aliquots of the reaction mixture were subjected to fluorescence spectroscopy and 30-μL aliquots were put into PCR tubes. The reaction tubes were then transferred into a DNA thermal cycler. Starting at 4 °C, the plate temperature was elevated at maximal speed to 37 °C. Incubation times ranged between 0 and 6 h as indicated in each figure. The reaction tubes were not agitated during the reaction. Five microliter aliquots from each tube in triplicate were subjected to fluorescence spectroscopy and the mean of the three measurements was determined. At the diluted concentration, CoQ_{10}, NDGA, and Myr did not compete with ThT for fAβ at either 4 °C or 37 °C for 1 min (data not shown).

Other analytical procedures. Protein concentrations of the supernatants of the reaction mixtures after centrifugation were determined by the method of Bradford [20] with a protein assay kit (Bio-Rad Laboratories, Hercules, CA). The Aβ(1–40) solution quantified by amino acid analysis was used as the standard. The statistical significance of the data was analyzed by the linear least squares fit. The effective concentration EC_{50} was defined as the concentration of CoQ_{10}, NDGA, or Myr to inhibit the formation or extension of fAβs to 50% of the control value, or the concentration to destabilize fAβs to 50% of the control value. EC_{50} was calculated by the sigmoidal curve fitting of the data, using Igor Pro ver.4 (WaveMetrics, Lake Oswego, OR, USA).

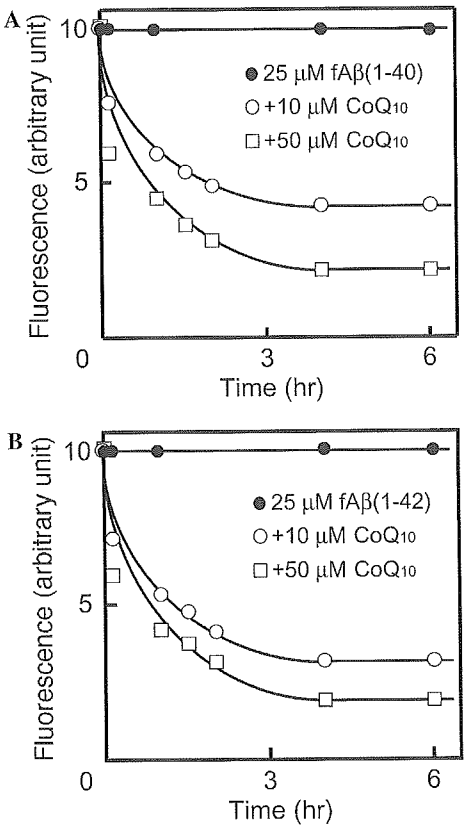

Fig. 2. Effects of CoQ_{10} on the kinetics of destabilization of fAβ(1–40) (A) and fAβ(1–42) (B). The reaction mixtures containing 25 μM fAβ(1–40) (A) or fAβ(1–42) (B), 50 mM phosphate buffer, pH 7.5, 100 mM NaCl, and 0 (●), 10 (○), or 50 μM (□) of CoQ_{10} were incubated at 37 °C for the indicated times. Each figure shows a representative pattern of three independent experiments.

Results and discussion

As shown in Figs. 1A and B, when fresh Aβ(1–40) or Aβ(1–42) was incubated at 37 °C, the fluorescence of ThT followed a characteristic sigmoidal curve. This curve is consistent with a nucleation-dependent polymerization model [3]. When Aβ(1–40) was incubated with 10 and 50 μM CoQ_{10}, the final equilibrium level decreased dose-dependently (Fig. 1A). A similar effect of CoQ_{10} was observed with Aβ(1–42) (Fig. 1B). As shown in Figs. 1C and D, when fresh Aβ(1–40) or Aβ(1–42) was incubated with fAβ(1–40) or fAβ(1–42), respectively, at 37 °C, the fluorescence increased hyperbolically without a lag phase and proceeded to equilibrium much more rapidly than without seeds (compare Figs. 1A and B with C and D). This curve is consistent with a first-order kinetic model [19]. When Aβ(1–40) and fAβ(1–40) were incubated with CoQ_{10}, the final equilibrium level decreased (Fig. 1C). A similar effect of CoQ_{10} was observed for the extension of fAβ(1–42) (Fig. 1D). We observed that 50 μM CoQ_{10} inhibited the extension of sonicated fAβ(1–40) and fAβ(1–42) electron-microscopically (data not shown).

As shown in Figs. 2A and B, the fluorescence of ThT was almost unchanged during the incubation of fresh fAβ(1–40) or fAβ(1–42) at 37 °C without additional molecules. On the other hand, the ThT fluorescence decreased immediately after addition of CoQ_{10} to the reaction mixture. After incubation of 25 μM fresh fAβ(1–40) with 50 μM CoQ_{10} for 1 h, many short, sheared fibrils were observed (Fig. 3B). At 6 h, the number of fibrils was reduced markedly, and small amorphous aggregates were occasionally observed (Fig. 3C). Similar morphology was observed when 25 μM fresh fAβ(1–42) was incubated with 50 μM CoQ_{10} (data not shown).

After incubation with 50 μM CoQ_{10} for 6 h, fAβ (1–40) and fAβ(1–42) were stained with Congo red much more weakly than fresh fAβ(1–40) and fAβ(1–42). However, they all showed orange-green birefringence under polarized light. This means that a significant amount of intact fAβ(1–40) and fAβ(1–42) still remains in the mixture after the reaction. When the protein concentration of the supernatant after centrifugation at 4 °C for 2 h at $1.6 \times 10^4 g$ was measured by the Bradford assay, no proteins were detected in the supernatant. This implies that although these agents could destabilize fAβ(1–40) and fAβ(1–42) to visible aggregates (Fig.

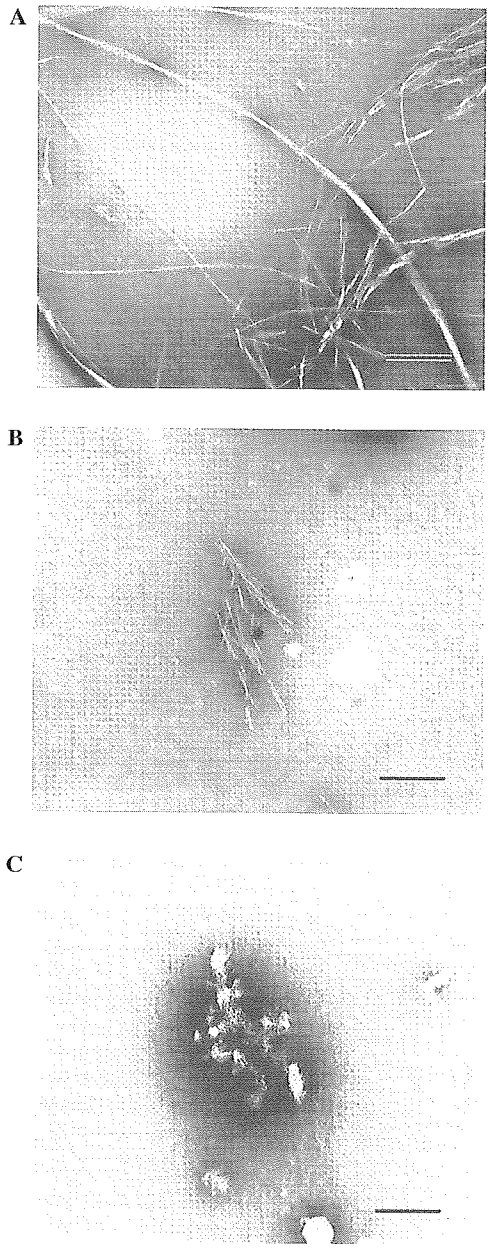

Fig. 3. Electron micrographs of destabilized fAβ(1–40). The reaction mixture containing 25 μM fAβ(1–40), 50 mM phosphate buffer, pH 7.5, 100 mM NaCl, and 50 μM CoQ_{10} was incubated at 37 °C for 0 h (A), 1 h (B) or 6 h (C). Scale bars indicate a length of 250 nm.

3C), they could not depolymerize fAβ(1–40) and fAβ(1–42) to monomers or oligomers of Aβ(1–40) and Aβ(1–42). When fresh 50 μM Aβ(1–40) or Aβ(1–42) was incubated with the pellet at 10 μg/mL, no increase in the fluorescence was observed for 6 h. This implies that destabilized fAβ(1–40) and fAβ(1–42) could not function as seeds.

We calculated EC_{50}, the concentrations of NDGA, Myr, or CoQ_{10} to inhibit the formation or extension of fAβs to 50% of the control value, or the concentrations to destabilize fAβs to 50% of the control value, by the sigmoidal curve fitting of the data as shown (Table 1). The overall activity of the molecules examined was in the order of: NDGA = Myr > CoQ_{10}.

In this study, we showed that CoQ_{10} dose-dependently inhibited fAβ formation from fresh Aβ, as well as destabilizing preformed fAβ in vitro. The anti-amyloidogenic and fibril-destabilizing effects of CoQ_{10} were slightly weaker than those of NDGA and Myr. Our previous systematic in vitro study indicated that the overall activity of the anti-amyloidogenic molecules may be in the order of: NDGA = wine-related polyphenols (Myr, morin, and quercetin) ≫ RIF = tetracyclines (TC) > poly(vinylsulfonic acid, sodium salt) = 1,3-propanedisulfonic acid, disodium salt > β-sheet breaker peptides (iAβ5) > nicotine [6,11,18]. Tomiyama et al. [21] suggested that RIF binds to Aβ by hydrophobic interactions between its lipophilic ansa chain and the hydrophobic region of Aβ, thus blocking the association between Aβ molecules that lead to fAβ formation. The anti-amyloidogenic activity of NDGA, TCs, small-molecule anionic sulfonates or sulfates, melatonin, iAβ5, and nicotine may also be related to the propensity to bind to the specific sites of Aβ [6,22–26]. Recently, we also showed that lipophilic vitamin, vitamin A, dose-dependently inhibits formation and extension of fAβ(1–40) and fAβ(1–42), as well as destabilizing preformed fAβs in vitro [12]. The overall activity of vitamin A and β-carotene was in the order of retinol = retinal > β-carotene > retinoic acid [12]. We speculated that the decrease in lipophilicity might reduce the binding affinity of retinoic acid to Aβ and/or fAβ to exhibit anti-amyloidogenic and fibril-destabilizing effects in vitro

Table 1
The effective concentrations (EC_{50}) of NDGA, Myr, and CoQ_{10} for the formation, extension, and destabilization of fAβ(1–40) and fAβ(1–42)

Compounds	Formation[a]		Extension[b]		Destabilization[c]	
	fAβ(1–40)	fAβ(1–42)	fAβ(1–40)	fAβ(1–42)	fAβ(1–40)	fAβ(1–42)
NDGA	0.21 μM	1.1 μM	0.22 μM	0.11 μM	0.99 μM	0.93 μM
Myr	0.37	0.51	0.17	0.16	1.8	0.95
CoQ_{10}	1.8	5.5	13	9.3	5.3	4.9

[a] The reaction mixtures containing 50 μM Aβ(1–40) or 25 μM Aβ(1–42), 50 mM phosphate buffer, pH 7.5, 100 mM NaCl, and 0, 0.01, 0.1, 1, 10, and 50 μM NDGA, Myr, or CoQ_{10} were incubated at 37 °C for 7 days and 24 h, respectively.

[b] The reaction mixtures containing 10 μg/mL (2.3 μM) sonicated fAβ(1–40) or fAβ(1–42), 50 μM Aβ(1–40) or Aβ(1–42), 50 mM phosphate buffer, pH 7.5, 100 mM NaCl, and 0, 0.01, 0.1, 1, 10, and 50 μM NDGA, Myr, or CoQ_{10} were incubated at 37 °C for 1 h.

[c] The reaction mixtures containing 25 μM fAβ(1–40) or fAβ(1–42), 50 mM phosphate buffer, pH 7.5, 100 mM NaCl, and 0, 0.01, 0.1, 1, 10, and 50 μM NDGA, Myr, or CoQ_{10} were incubated at 37 °C for 6 h.

[13]. Interestingly, CoQ_{10}, NDGA, wine-related polyphenols, RIF, melatonin, nicotine, and vitamin A have all been reported to have antioxidant activity [9,13,21,24,27,28]. CoQ_{10} with potent lipophilic and antioxidant motifs could bind specifically to Aβ and/or fAβ, inhibit fAβ formation, and/or destabilize preformed fAβ. Moreover, CoQ_{10} may prevent the development of AD, not only through scavenging reactive oxygen species, but also through directly inhibiting the deposition of fAβ in the brain. Although the exact mechanism of anti-amyloidogenic activity of CoQ_{10} is unclear, these compounds could be key molecules for the development of therapeutics for AD. Further studies, such as nuclear magnetic resonance experiments, are essential to reveal the exact structure–activity relationships for the antioxidants and other organic compounds which exhibit anti-amyloidogenic and fibril-destabilizing effects.

Acknowledgments

The authors thank Drs. Souichi Okino and Kazuo Iwasa (Kanazawa University) for cooperation in the experiments. This work was supported in part by a Grant-in-Aid for Scientific Research (M.Y.), a grant for the 21st Century COE Program (on Innovative Brain Science for Development, Learning and Memory) (M.Y.), a grant for the Knowledge Cluster Initiative [High-Tech Sensing and Knowledge Handling Technology (Brain Technology)] (M.Y.) and a Grant-in-Aid for Scientific Research on Priority Areas (C)—Advanced Brain Science Project (H.N.) from the Japanese Ministry of Education, Culture, Sports, Science and Technology, Japan, and a grant to the Amyloidosis Research Committee from the Ministry of Health, Labour, and Welfare, Japan (M.Y.).

References

[1] C. Haass, B. De Strooper, The presenilins in Alzheimer's disease-proteolysis holds the key, Science 286 (1999) 916–919.
[2] D.J. Selkoe, Alzheimer's disease is a synaptic failure, Science 298 (2002) 789–791.
[3] J.T. Jarrett, P.T. Lansbury Jr., Seeding "one-dimensional crystallization" of amyloid: a pathogenic mechanism in Alzheimer's disease and scrapie?, Cell 73 (1993) 1055–1058.
[4] H. Naiki, F. Gejyo, Kinetic analysis of amyloid fibril formation, Methods Enzymol. 309 (1999) 305–318.
[5] H. Naiki, K. Hasegawa, I. Yamaguchi, H. Nakamura, F. Gejyo, K. Nakakuki, Apolipoprotein E and antioxidants have different mechanisms of inhibiting Alzheimer's beta-amyloid fibril formation in vitro, Biochemistry 37 (1998) 17882–17889.
[6] K. Ono, K. Hasegawa, Y. Yoshiike, A. Takashima, M. Yamada, H. Naiki, Nordihydroguaiaretic acid potently breaks down preformed Alzheimer's beta-amyloid fibrils in vitro, J. Neurochem. 81 (2002) 434–440.
[7] D. Pratico, N. Delanty, Oxidative injury in diseases of the central nervous system: focus on Alzheimer's disease, Am. J. Med. 109 (2000) 577–585.
[8] R. Subramaniam, T. Koppal, M. Green, S. Yatin, B. Jordan, J. Drake, D.A. Butterfield, The free radical antioxidant vitamin E protects cortical synaptosomal membranes from amyloid beta-peptide(25–35) toxicity but not from hydroxynonenal toxicity: relevance to the free radical hypothesis of Alzheimer's disease, Neurochem. Res. 23 (1998) 1403–1410.
[9] Y. Goodman, M.R. Steiner, S.M. Steiner, M.P. Mattson, Nordihydroguaiaretic acid protects hippocampal neurons against amyloid beta-peptide toxicity, and attenuates free radical and calcium accumulation, Brain Res. 654 (1994) 171–176.
[10] T. Kihara, S. Shimohama, H. Sawada, J. Kimura, T. Kume, H. Kochiyama, T. Maeda, A. Akaike, Nicotinic receptor stimulation protects neurons against beta-amyloid toxicity, Ann. Neurol. 42 (1997) 159–163.
[11] K. Ono, Y. Yoshiike, A. Takashima, K. Hasegawa, H. Naiki, M. Yamada, Potent anti-amyloidogenic and fibril-destabilizing effects of polyphenols in vitro: implications for the prevention and therapeutics of Alzheimer's disease, J. Neurochem. 87 (2003) 172–181.
[12] K. Ono, Y. Yoshiike, A. Takashima, K. Hasegawa, H. Naiki, M. Yamada, Vitamin A exhibits potent antiamyloidogenic and fibril-destabilizing effects in vitro, Exp. Neurol. 189 (2004) 380–392.
[13] L. Ernster, G. Dallner, Biochemical, physiological and medical aspects of ubiquinone function, Biochim. Biophys. Acta 1271 (1995) 195–204.
[14] M. Soderberg, C. Edlund, I. Alafuzoff, K. Kristensson, G. Dallner, Lipid composition in different regions of the brain in Alzheimer's disease/senile dementia of Alzheimer's type, J. Neurochem. 59 (1992) 1646–1653.
[15] F. de Bustos, J.A. Molina, F.J. Jimenez-Jimenez, A. Garcia-Redondo, C. Gomez-Escalonilla, J. Porta-Etessam, A. Berbel, M. Zurdo, B. Barcenilla, G. Parrilla, R. Enriquez-de-Salamanca, J. Arenas, Serum levels of coenzyme Q10 in patients with Alzheimer's disease, J. Neural. Transm. 107 (2000) 233–239.
[16] M. Imagawa, S. Naruse, S. Tsuji, A. Fujioka, H. Yamaguchi, Coenzyme Q10, iron, and vitamin B6 in genetically confirmed Alzheimer's disease, Lancet 340 (1992) 671.
[17] K. Hasegawa, I. Yamaguchi, S. Omata, F. Gejyo, H. Naiki, Interaction between A beta(1–42) and A beta(1–40) in Alzheimer's beta-amyloid fibril formation in vitro, Biochemistry 38 (1999) 15514–15521.
[18] K. Ono, K. Hasegawa, M. Yamada, H. Naiki, Nicotine breaks down preformed Alzheimer's beta-amyloid fibrils in vitro, Biol. Psychiatry 52 (2002) 880–886.
[19] H. Naiki, K. Nakakuki, First-order kinetic model of Alzheimer's beta-amyloid fibril extension in vitro, Lab. Invest. 74 (1996) 374–383.
[20] M.M. Bradford, A rapid and sensitive method for the quantitation of microgram quantities of protein utilizing the principle of protein-dye binding, Anal. Biochem. 72 (1976) 248–254.
[21] T. Tomiyama, A. Shoji, K. Kataoka, Y. Suwa, S. Asano, H. Kaneko, N. Endo, Inhibition of amyloid beta protein aggregation and neurotoxicity by rifampicin. Its possible function as a hydroxyl radical scavenger, J. Biol. Chem. 271 (1996) 6839–6844.
[22] G. Forloni, L. Colombo, L. Girola, F. Tagliavini, M. Salmona, Anti-amyloidogenic activity of tetracyclines: studies in vitro, FEBS Lett. 487 (2001) 404–407.
[23] R. Kisilevsky, L.J. Lemieux, P.E. Fraser, X. Kong, P.G. Hultin, W.A. Szarek, Arresting amyloidosis in vivo using small-molecule anionic sulphonates or sulphates: implications for Alzheimer's disease, Nat. Med. 1 (1995) 143–148.
[24] M. Pappolla, P. Bozner, C. Soto, H. Shao, N.K. Robakis, M. Zagorski, B. Frangione, J. Ghiso, Inhibition of Alzheimer beta-fibrillogenesis by melatonin, J. Biol. Chem. 273 (1998) 7185–7188.

[25] C. Soto, M.S. Kindy, M. Baumann, B. Frangione, Inhibition of Alzheimer's amyloidosis by peptides that prevent beta-sheet conformation, Biochem. Biophys. Res. Commun. 226 (1996) 672–680.

[26] H. Zeng, Y. Zhang, L.-J. Peng, H. Shao, N.K. Menon, J. Yang, A.R. Salomon, R.P. Freidland, M.G. Zagorski, Nicotine and amyloid formation, Biol. Psychiatry 49 (2001) 248–257.

[27] W. Linert, M.H. Bridge, M. Huber, K.B. Bjugstad, S. Grossman, G.W. Arendash, In vitro and in vivo studies investigating possible antioxidant actions of nicotine: relevance to Parkinson's and Alzheimer's diseases, Biochim. Biophys. Acta 1454 (1999) 143–152.

[28] L. Tesoriere, M. Ciaccio, A. Bongiorno, A. Riccio, A.M. Pintaudi, M.A. Livrea, Antioxidant activity of all-*trans*-retinol in homogeneous solution and in phosphatidylcholine liposomes, Arch. Biochem. Biophys. 307 (1993) 217–223.

特集 レビー小体型痴呆

レビー小体型痴呆の画像診断

Imaging for clinical diagnosis of dementia with Lewy bodies

金沢大学医学部附属病院神経内科
Mitsuhiro Yoshita 吉田光宏

金沢大学大学院医学系研究科
脳老化・神経病態学(神経内科学)教授
Masahito Yamada 山田正仁

Summary

レビー小体型痴呆(DLB)の診断における画像・機能検査の有用性について概説した。DLBでは，脳核磁気共鳴画像(MRI)における側頭葉内側および被殻の萎縮，ポジトロン放射断層撮影法(PET)では，^{18}F-フルオロデオキシグルコースによる後頭葉の糖代謝低下，および^{18}F-DOPAによる線条体の取り込み低下，^{123}I-IMP，^{99m}Tc-HMPAO，^{99m}Tc-ECDの各核種による脳血流の単一光子放射コンピュータ断層撮影法(SPECT)における後頭葉脳血流低下，^{123}I-メタ-ヨードベンジルグアニジン(MIBG)心筋シンチグラフィにおける交感神経節後機能の低下などが報告されている。DLBとアルツハイマー病との鑑別診断における，それらの感度と特異度について比較検討した。

Key words

- レビー小体型痴呆
- 脳核磁気共鳴画像(MRI)
- ポジトロン放射断層撮影法(PET)
- 単一光子放射コンピュータ断層撮影法(SPECT)
- ^{123}I-メタ-ヨードベンジルグアニジン(MIBG)心筋シンチグラフィ

Ⅰ はじめに

レビー小体型痴呆(dementia with Lewy bodies；DLB)の臨床診断基準は，第1回のDLBの国際ワークショップの報告として出版されたものが現在用いられている[1]。この診断基準では，特異度は高いが，感度が低い点が問題となっている[2]。本稿では画像検査がどの程度DLBの診断に寄与できるかという点について，アルツハイマー病(AD)との鑑別を中心に検討した。

Ⅱ 脳核磁気共鳴画像(MRI)

通常のMRI(magnetic resonance imaging)は，進行性核上性麻痺，皮質基底核萎縮症，多発性脳梗塞などの他のパーキンソニズムと痴呆をきたす疾患とDLBとの鑑別に有用な場合がある。

ADとの比較では，病理で内側側頭葉萎縮(medial temporal lobe atrophy；MTA)がADに比し，DLBで軽いことが報告され[3]，MRIでもその点が検討されている[4,5]。Hashimotoらは，臨床診断のついた27名のDLB患者とAD患者および健常対照者(NC)の海馬の萎縮の程度をMRIの冠状断で比較した結果，ADの海馬萎縮が最も強く，DLBのそれはADとNCの中間であり，海馬萎縮の程度を比較することはADとDLBの鑑別に有用であるとした[4]。

O'Brienらニューキャッスルのグループは，MRIでMTAをvisual rating scaleを用いて検討し，DLBではMTAのないことが，DLBとADおよび脳血管性痴呆(VaD)との鑑別に役立つと述べている[5]。特異度はそれぞれ100%と88%と高かったが，感度はともにわずか38%であった。さらに彼らは，MRIで被殻の萎縮の程度を，DLB，AD，NCで比較検討し，AD，NCに比してDLBで有意に被殻の萎縮が強く，DLBのパーキンソニズムとの関連を推測している[6]。

Molinaらは，プロトン核磁気共鳴スペクトロスコピー(proton magnetic resonance spectroscopy；^{1}H-MRS)では，半卵円中心の白質のN-アセチルアスパルテート(N-acetyl aspartate；NAA)，クレアチン+クレアチンリン酸塩(creatine+phosphocreatine；Cr)，コリン含有物質(Cho)，グルタメート/グルタミン(glutamate/glutamine；Glx)を測定し，NAA/Cr，Glx/Cr，Cho/Crの比が，NCに対し有意に低いことを報告し，DLBの生前診断に役立つと報告している[7]。

Ⅲ ポジトロン放射断層撮影法(PET)

^{18}F-フルオロデオキシグルコース(fluorodeoxyglucose；FDG)とPET(positron emission tomography)によるグルコース代謝の測定は，脳代謝画像の代表である。三次元撮像法や画像解析技術の進歩により，DLBとADが異なった皮質糖代謝を示すことが明らかになった。Ishiiらは，臨床診断されたAD，DLB，NCを各12名ずつFDG-PETを用いて局所脳糖代謝の比(cerebral metabolic rate of glucose；CMRglc)を検討した[8]。CMRglcの低下パターンをみると，頭頂側頭連合野の低下はADとDLBとで類似していたが，低下の程度はDLBでより大きかった。さらに，後頭葉の糖代謝の低下がDLBでしばしばみられ，probable DLBとprobable ADの比較では，感度，特異度とも92%と診断に有用であった。Higuchiらは，FDG-PETで一次視覚野の代謝低下に注目すると，感度86%，特異度91%でprobable ADからprobable DLBを鑑別可能であったと報告している[9]。Minoshimaらは，FDG-PETを用いて病理診断のついた11名のDLBと10名のADの脳の糖代謝を検討し，後頭葉，特に一次視覚野の糖代謝の低下を指標とした場合，90%の感度と80%の特異度をもってDLBとADを鑑別できたと報告している[10]。

^{18}F-6-フルオロドーパ(^{18}F-DOPA)は，ドパミンニューロン終末に取り込まれたのち，ドーパ脱炭酸酵素により^{18}F-ドパミンへと代謝され，シナプス小胞に蓄えられる。線条体での^{18}F-DOPA PETは，機能しているドパミンニューロン終末の数とそのドパミン貯蔵能力を推測することができることから，パーキンソン病(PD)の診断や経過観察に用いる脳機能画像法として中心的な役割を果たしてきた。Huらは，^{18}F-DOPA PETを用いDLB 7名(probable 6，definite 1)，probable AD 10名，NC 10名で検討し，被殻の^{18}F-DOPAの取り込み率低下を指標とした場合，100%の特異度と，85%の感度でDLBをADから鑑別可能であったと報告した[11]。他のドパミン代謝画像としては，シナプス小胞のモノアミントランスポーターのマーカーである^{11}C-ジヒドロテトラベナジン(dihydrotetrabenazine；DTBZ)によるPETを用いたGilmanらの報告があり，ADとDLBの鑑別に有用としている[12]。

アセチルコリンエステラーゼ(AChE)活性を測定するためのPET製剤^{11}C-N-メチル-4-ピペリジルアセテート(methyl-4-piperidyl acetate；MP4A)が開発されAD，DLBで検討されているが，DLBの診断における有用性は確立していない。Shinotohらは，ADでAChE活性が，新皮質，海馬，扁桃体で低下していることを報告している[13]。一方，Herholzは，DLBの後頭葉でAChE活性が著明に低下している83歳女性例を報告した[14]。今後多数例での検討が待たれる。

Ⅳ 単一光子放射コンピュータ断層撮影法(SPECT)

脳血流SPECT(single-photon emission computed tomography)によるADとDLBの比較では，Ishiiらは^{123}I-ヨードアンフェタミン(iodoamphetamine；IMP)SPECTを各14名のNC，probable DLB，probable AD

に対して行い，画像統計解析法の1つであるstatistical parametric mapping(SPM) 95で解析し，DLB群でAD群に対し有意に後頭葉の血流が低下していることを報告した[15]。DLBの診断における脳血流SPECTの有用性については，Lobotesisらは，AD 50名(definite 2, probable 21, possible 27)，DLB 23名(definite 4, probable 17, possible 2)を^{99m}Tc-ヘキサメチルプロピレンアミンオキシム(hexamethyl propylene amine oxime；HMPAO) SPECTで検討し，後頭葉の血流低下をDLBの診断の指標とした場合，特異度は86%であったが，感度は64%と低かったことを報告した[16]。Varmaらは，同様の検討を行い感度64%，特異度76%と報告している[17]。

筆者らは，Matsudaらが開発したSPECT画像解析ソフトeazy Z-score imaging system(eZIS)[18]を用いて，probable AD 23名とprobable DLB 24名の^{99m}Tc-エチルシステイン酸ダイマー(ethyl cysteinate dimer；ECD) SPECTによる後頭葉の一次視覚野の脳血流の低下の有無を検討した[19]。AD，DLBの両群からDLBを診断する感度および特異度を検討すると，後頭葉の一次視覚野での血流低下のZスコアが1～6を異常とした場合，感度は91%，特異度は33%であり，一方Zスコアが2～6を異常とした場合，感度は65%，特異度は95%であった。Zスコアが2～6を異常とした場合，Lobotesisらの報告[16]より感度は大差ないが，特異度は高かった。図1にADとDLBのeZIS画像を示す。

現時点では，日本でまだ使えないが，線条体のドパミントランスポーター量を評価するSPECT用の核種として^{123}I-β-カルボキシヨードフェニルトロパン(2β-carboxymethoxy-3β-[4-iodophenyl]tropane；β-CIT)，^{123}I-β-カルボキシヨードフェニルフルオロピルノルトロパン[2β-carbomethoxy-3β-(4-iodophenyl)-N-(3-fluoropropyl) nortropane；FP-CIT]があり，これらを用いたSPECTでDLBの線条体では集積低下がみられることから，ADとDLBの鑑別に有用との報告がある[20][21]。Donnemillerらは，NC 3名，probable AD 6名，probable DLB 7名で^{123}I-β-CIT SPECTを行い，線条体の集積を検討し，DLBはAD，NCから鑑別可能であったと報告している[30]。O'Brienらは，NC 33名，probable AD 34名，DLB 23名(probable 17, possible 6)，PD 38名，痴呆を伴うPD(Parkinson's disease with dementia；PDD) 36名を対象に^{123}I-FP-CIT SPECTを実施し，線条体でのドパミントランスポーターの減少を検討した[21]。その結果，感度は78%，特異度は94%，陽性反応的中度は90%で，ADからDLBを鑑別可能であったが，PD，PDDとDLBの鑑別は困難であったと報告している。

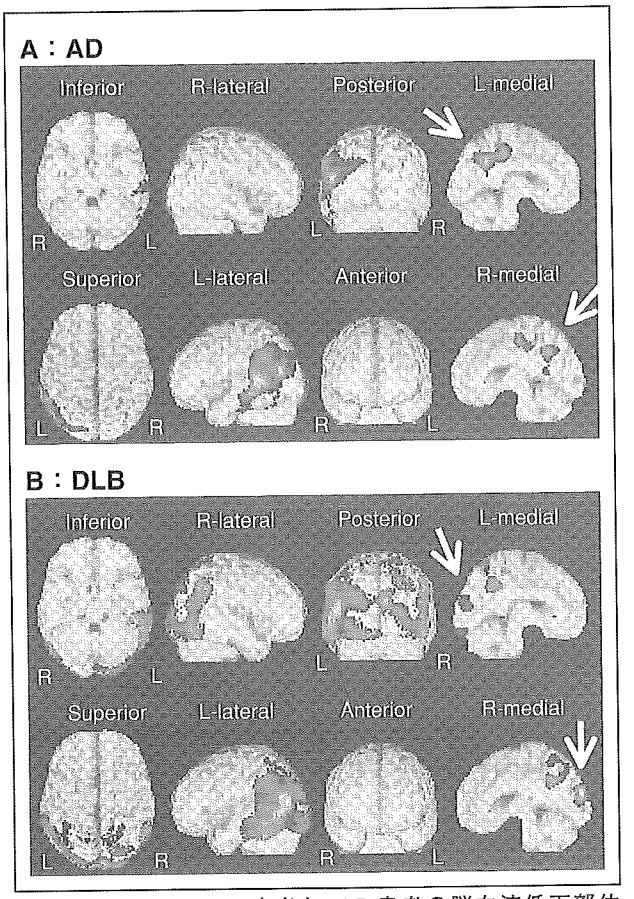

図1　eZISによるAD患者とDLB患者の脳血流低下部位
(巻頭グラビアページ参照)
コントロール群と比較し，Zスコアが2≦Z≦6の範囲を視覚化している。AD患者(A)では，後部帯状回および左側頭葉から頭頂葉後頭葉移行部で脳血流低下を認める。DLB患者(B)では，AD患者で認められる脳血流低下部位に加え，後頭葉の視覚野で血流低下を認める。

O'Brienらは，ムスカリン性アセチルコリン受容体(mAChR)のイメージング製剤の1つである^{123}I-キヌクリジニルベンジレート(quinuclidinyl benzilate；QNB)を

用いて，AD，DLB，PDD，NCでmAChRの評価を行い，画像統計解析法SPM 99を用いて検討した[22]。ADでは，前頭葉，後頭葉，側頭後頭葉で^{123}I-QNBの集積低下を認めたが，一方DLBとPDDでは，後頭葉で集積の上昇を認め，ADとDLBの鑑別に有用であるとした。

Ⅴ ^{123}I-メタ-ヨードベンジルグアニジン(MIBG)心筋シンチグラフィ

PDを含むレビー小体病における^{123}I-MIBG(meta-iodobenzylguanidine)の心筋への取り込み低下については，本邦やドイツを中心に多くの論文が発表されてきた[23]。

DLBにおいてもPDと同様に^{123}I-MIBGの心筋への取り込み低下がみられ，ADとの鑑別に有用である[24)-26)]。^{123}I-MIBGの心筋への取り込みは，プラナー正面像で心臓および縦隔の各関心領域の平均カウントの比率である心・縦隔比(H/M比)を求め半定量化する。われわれの検討では，^{123}I-MIBG心筋シンチグラフィで，^{123}I-MIBG静注3時間後に撮像された後期像におけるH/M比が，1.5未満を陽性とした場合，DLBをADから鑑別する感度は96%，特異度は100%であった[19)24)]。図2にADとDLBの^{123}I-MIBG心筋シンチグラフィのプラナー正面像を提示する。

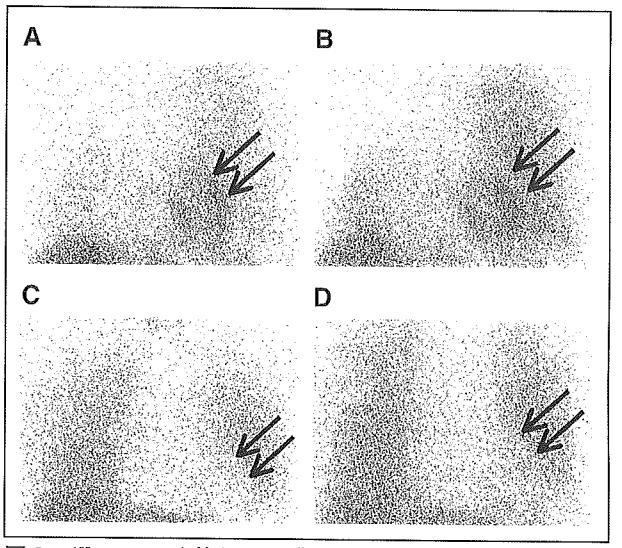

図2 ^{123}I-MIBG心筋シンチグラフィ
AD患者では，正常に集積を示すが(A,B)，DLB患者では初期像，後期像ともにMIBGの心筋への集積を認めない(C,D)。
A：AD患者の初期像，B：AD患者の後期像，C：DLB患者の初期像，D：DLB患者の後期像
初期像：^{123}I-MIBG静注20分後のプラナー正面像，後期像：^{123}I-MIBG静注3時間後のプラナー正面像

Ⅵ まとめ

各種画像診断においてDLBを主にADから鑑別する場合の感度，特異度を中心にまとめた。一定の傾向はみられるものの，それぞれの感度，特異度は，報告によりばらつきがある。これにはDLBがしばしばAD病変と共存していること，対象患者の重症度，進行度による違い，診断の質の違い[臨床診断(possibleあるいはprobable)か，病理診断(definite)か]，症例数，検討方法などが影響しているものと思われる。

臨床情報に加え，これら画像検査から得られる情報を加味することでDLBの診断精度を上げることができる。なかでも^{123}I-MIBG心筋シンチグラフィがDLBの診断において感度，特異度とも高い。痴呆性疾患の検査では脳に注目が行きがちであるが，DLBは中枢神経系から末梢の自律神経系まで幅広く，臨床的にも神経病理学的にも異常を認める疾患であり，このような観点からのアプローチも大切であると考えられる[27]。

PETやSPECTカメラで使用可能な新しいプローブの開発も進んでいる。今後，画像所見と病理所見がどのように関連しているかを前方視的研究によって綿密に検討していくことが，DLBを正確に診断するうえでの画像検査の有用性を検証していくために重要と考えられる。

文 献

1) McKeith IG, Galasko D, Kosaka K, et al：Consensus guidelines for the clinical and pathological diagnosis of dementia with Lewy bodies(DLB)；Report of the consortium on DLB international workshop. Neurology 47：1113-1124, 1996
2) McKeith IG, Mintzer J, Aarsland D, et al：Dementia

with Lewy bodies. Lancet Neurol **3** : 19-28, 2004
3) Lippa CF, Smith TW, Swearer JM : Alzheimer's disease and Lewy body disease ; A comparative clinicopathological study. Ann Neurol **35** : 81-88, 1994
4) Hashimoto M, Kitagaki H, Imamura T, et al : Medial temporal and whole-brain atrophy in dementia with Lewy bodies. A volumetric MRI study. Neurology **51** : 357-362, 1998
5) Barber R, Gholkar A, Scheltens P, et al : Medial temporal lobe atrophy on MRI in dementia with Lewy bodies. Neurology **52** : 1153-1158, 1999
6) Cousins DA, Burton EJ, Burn DJ, et al : Atrophy of the putamen in dementia with Lewy bodies but not Alzheimer's disease. An MRI study. Neurology **61** : 1191-1195, 2003
7) Molina JA, Garcia-Segura JM, Benito-Leon J, et al : Proton magnetic resonance spectroscopy in dementia with Lewy bodies. Eur Neurol **48** : 158-163, 2002
8) Ishii K, Imamura T, Sasaki M, et al : Regional cerebral glucose metabolism in dementia with Lewy bodies and Alzheimer's disease. Neurology **51** : 125-130, 1998
9) Higuchi M, Tashiro M, Arai H, et al : Glucose hypometabolism and neuropathological correlates in brains of dementia with Lewy bodies. Exp Neurol **162** : 247-256, 2000
10) Minoshima S, Foster NL, Shima AA, et al : Alzheimer's disease versus dementia with Lewy bodies ; Cerebral metabolic distinction with autopsy confirmation. Ann Neurol **50** : 358-365, 2001
11) Hu XS, Okamura N, Arai H, et al : ^{18}F-fluorodopa PET study of striatal dopamine uptake in the diagnosis of dementia with Lewy bodies. Neurology **55** : 1575-1577, 2000
12) Gilman S, Koeppe RA, Little R, et al : Striatal monoamine terminals in Lewy body dementia and Alzheimer's disease. Ann Neurol **55** : 774-780, 2004
13) Shinotoh H, Namba H, Fukushi K, et al : Progressive loss of cortical acetylcholinesterase activity in association with cognitive decline in Alzheimer's disease ; A positoron emission tomography study. Ann Neurol **48** : 194-200, 2000
14) Herholz K : PET studies in dementia. Ann Nucl Med **17** : 79-89, 2003
15) Ishii K, Yamaji S, Kitagaki H, et al : Regional cerebral blood flow difference between dementia with Lewy bodies and AD. Neurology **53** : 413-416, 1999
16) Lobotesis K, Fenwick JD, Phipps A, et al : Occipital hypoperfusion on SPECT in dementia with Lewy bodies but not AD. Neurology **56** : 643-649, 2001
17) Varma AR, Talbot PR, Snowden JS, et al : ^{99m}Tc-HMPAO SPECT study of Lewy body disease. J Neurol **244** : 349-359, 1997
18) Matsuda H, Mizumura S, Soma T, et al : Conversion of brain SPECT images between different collimators and reconstruction processes for analysis using statistical parametric mapping. Nucl Med Commun **25** : 67-74, 2004
19) Yoshita M, Yamada M : Occipital cerebral hypoperfusin and cardiac sympathetic dysfunction in dementia with Lewy bodies and dementia of the Alzheimer's type. Neurology **60** : A208, 2003
20) Donnemiller E, Heilmann J, Wenning GK, et al : Brain perfusion scintigraphy with ^{99m}Tc-HMPAO or ^{99m}Tc-ECD and ^{123}I-beta-CIT single-photon emission tomography in dementia of the Alzheimer-type and diffuse Lewy body disease. Eur J Nucl Med **24** : 320-325, 1997
21) O'Brien JT, Colloby S, Fenwick J, et al : Dopamine transporter loss visualized with FP-CIT SPECT in the differential diagnosis of dementia with Lewy bodies. Arch Neurol **61** : 919-925, 2004
22) O'Brien JT, Colloby S, Pakrasi S, et al : ^{123}I-QNB SPECT demonstrates loss of cholinergic muscarinic receptors in Alzheimer's disease, but occipital increases in dementia with Lewy bodies and Parkinson's disease dementia. The 9th International Conference on Alzheimer's Disease and Related Disorders, poster No. 2-147, Philadelphia, 2004 Jul.
23) Yoshita M : Differentiation of idiopathic Parkinson's disease from striatonigral degeneration and progressive supranuclear palsy using iodine-123 meta-iodobenzylguanidine myocardial scintigraphy. J Neurol Sci **155** : 60-67, 1998
24) Yoshita M, Taki J, Yamada M : A clinical role for [^{123}I] MIBG myocardial scintigraphy in the distinction between dementia of the Alzheimer's-type and dementia with Lewy bodies. J Neurol Neurosurg Psychiatry **71** : 583-588, 2001
25) Watanabe H, Ieda T, Katayama T, et al : Cardiac ^{123}I-meta-iodobenzylguanidine (MIBG) uptake in dementia with Lewy bodies ; Comparison with Alzheimer's disease. J Neurol Neurosurg Psychiatry **70** : 781-783, 2001
26) Oide T, Tokuda T, Momose M, et al : Usefulness of [^{123}I] metaiodobenzylguanidine myocardial scintigraphy in differentiating between Alzheimer's disease and dementia with Lewy bodies. Intern Med **42** : 686-690, 2003
27) Baker RA : Getting to the heart of dementia. J Neurol Neurosurg Psychiatry **71** : 571-575, 2001

アルツハイマー病の血管病理

Vascular pathology in Alzheimer's disease

坂井　健二　Kenji SAKAI
教授　山田　正仁　Masahito YAMADA

金沢大学大学院医学系研究科脳老化・神経病態学(神経内科)

KEY WORDS

Alzheimer's disease
cerebral amyloid angiopathy
arteriosclerosis
white matter lesion
cerebral infarct

SUMMARY

アルツハイマー病(AD)は進行性の痴呆をきたす変性疾患で，病理学的には神経細胞脱落と老人斑，神経原線維変化の出現を特徴とするが，アミロイドアンギオパチー，細動脈硬化などの血管病変，脳梗塞や大脳白質病変などの血管性脳病変がADに高率に合併し，ADの病態に大きな影響を与えていることが近年注目されている．ADに関わる血管因子及びその作用機序の解明は、ADの発症や進行を予防する上で重要な課題である．

はじめに

アルツハイマー病(AD)は高齢者の痴呆の主要な原因であり，記憶を中心に高次脳機能が進行性に障害される神経変性疾患である[1]．ADの神経病理学的所見は，細胞外のアミロイドβ蛋白(Aβ)の沈着である老人斑(senile plaque：SP)，過剰にリン酸化されて難溶性となったタウ蛋白からなる神経原線維変化(neurofibrillary tangle：NFT)，神経細胞やシナプスの脱落を特徴とする[1]．近年，ADではSPやNFTに加えて，脳アミロイドアンギオパチー(cerebral amyloid angiopathy：CAA)や細動脈硬化などの血管病変や脳梗塞，脳出血，大脳白質病変などの血管性脳病変が高率に見られることが報告され，それらの病変がADの発症や進行，痴呆に関与している可能性が議論されている[2]．本稿では，ADに見られる血管病変について病理学的側面より概説し，ADの発症や病態への関与について考察したい．

脳アミロイドアンギオパチー

1．CAAの分類

CAAは脳血管へのアミロイド沈着症である[3]．沈着するアミロイド蛋白として6種類が知られており，アミロイド蛋白の種類とそれに対応する臨床病型により分類されている[3]．そのうち，高齢者やAD患者で認められるのはAβが沈着する孤発性Aβ型CAAであり，脳出血などの脳血管障害の原因になる[4]．

2．CAAの頻度

CAAは加齢に伴ってその頻度が増加し，60歳以上では約半数，90歳以上では約74%にCAAが認められたとの報告がある[5]．ADについては70～98%もの高率に認められ[2)5)-8)]ADでは脳実質だけでなく脳血管のAβ沈着も促進されている．

3．CAAの病理

光学顕微鏡的に[9)-11)]，CAAは主に大脳の髄膜と皮質の小動脈や細動脈に見られ(図1a，b)，後頭葉で最も高率に見られるが，大脳基底核，視床，脳幹や白質にはほとんど見られない．また，静脈や毛細血管にも時には沈着が見られる．軽度の場合には髄膜及び皮質表層の小動脈のごく一部にアミロイドの沈着が認められるのみであるが，高度の場合にはほとんどの小動脈や細動脈に高度のアミロイド沈着が認められる．アミロイドの沈着はまず平滑筋の基底膜に認められ，進行性に平滑筋細胞の変性が生じ，最終的に血管の内皮細胞を残して血管壁全体がアミロイドへ置き換わる．毛細血管，時に細動脈に沈着したアミロイドは周囲のニューロピルに滲み出したような形態を示し，タウ陽性変性神経突起を伴う(血管周囲性SP，drusige Entartung，図1c，d)．

電子顕微鏡的には[9)10)]，8～10nmのアミロイド線維が血管内腔から離れた部位の平滑筋細胞の基底膜に沈着し始め，内弾性板の方向へと拡大し，沈着の増加に伴って平滑筋細胞が変性する(図2)．

CAAが沈着した血管には血管壁の重複化，内膜の閉塞性変化やヒアリン化，微小動脈瘤様の拡張，フィブリノイド壊死などの二次性変化(CAA-associated vasculopathies)が認められ，これらの病変は脳葉型脳出血などのCAA関連脳血管障害の基盤となる(図3)[11)]．CAAが炎症を随伴し，血管炎を生じる場合もある[2)9)]．

4．CAAの生化学と沈着機序[9)12)13)]

ADや高齢者で見られるCAAの主成分はAβであり，更にアミロイドPコンポーネント，アポリポ蛋白E(ApoE)，シスタチンCなどの蛋白が共存している．Aβの C末端には異質性があり，アミノ酸が40位で終わるAβ40，42位で終わるAβ42の2つの主な分子種がある．SPのアミロイドがAβ42を主成分とするのに対し，CAAの主成分はAβ40である．

Aβの沈着機序については，最初にアミロイド前駆体蛋白(APP)が産生され，蛋白分解を受けてAβとなり，重合してアミロイド細線維として沈着する．APPは血管平滑筋細胞，神経細胞他の様々な細胞によって産生されるが，平滑筋細胞を欠く毛細血管壁にアミロイド沈着を認めることや，ヒトAPPを

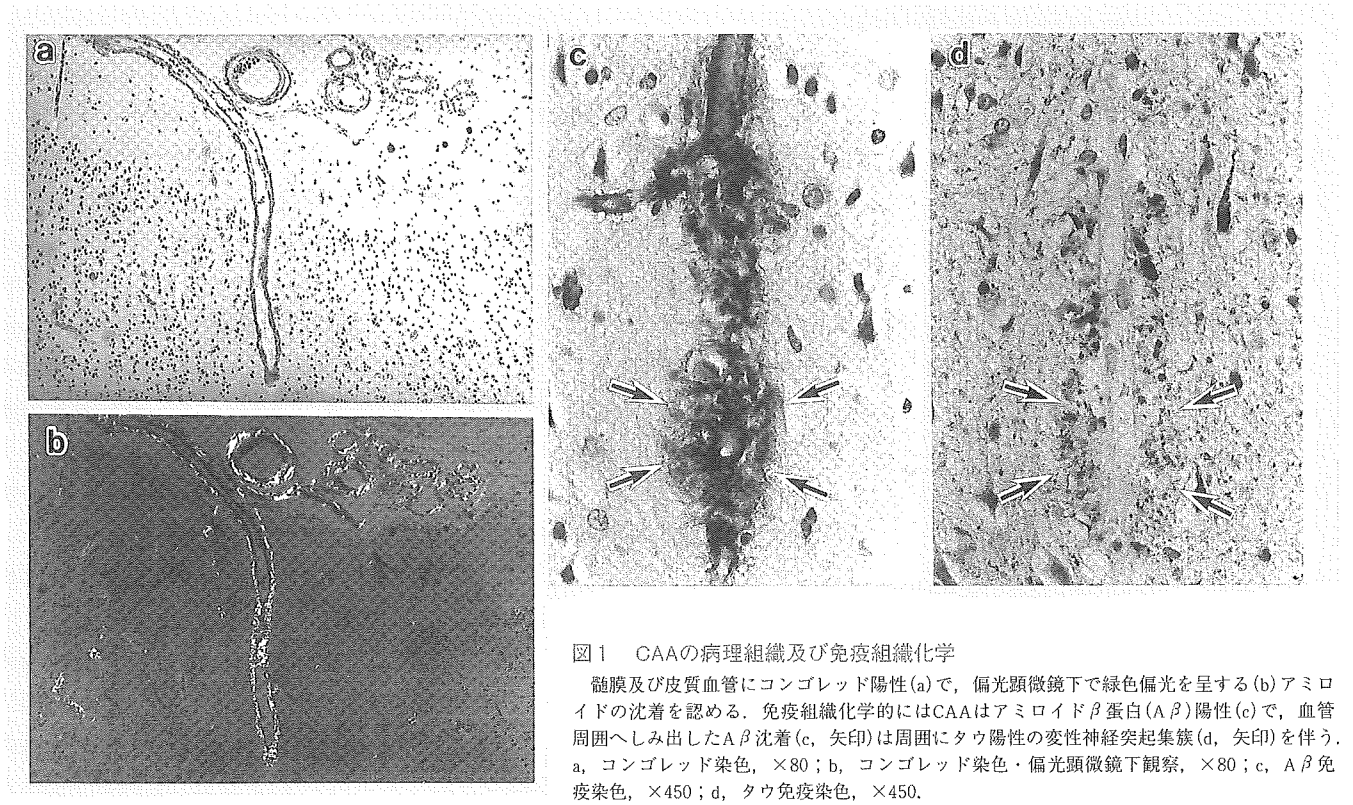

図1　CAAの病理組織及び免疫組織化学

髄膜及び皮質血管にコンゴレッド陽性(a)で，偏光顕微鏡下で緑色偏光を呈する(b)アミロイドの沈着を認める．免疫組織化学的にはCAAはアミロイドβ蛋白(Aβ)陽性(c)で，血管周囲へしみ出したAβ沈着(c，矢印)は周囲にタウ陽性の変性神経突起集簇(d，矢印)を伴う．a，コンゴレッド染色，×80；b，コンゴレッド染色・偏光顕微鏡下観察，×80；c，Aβ免疫染色，×450；d，タウ免疫染色，×450．

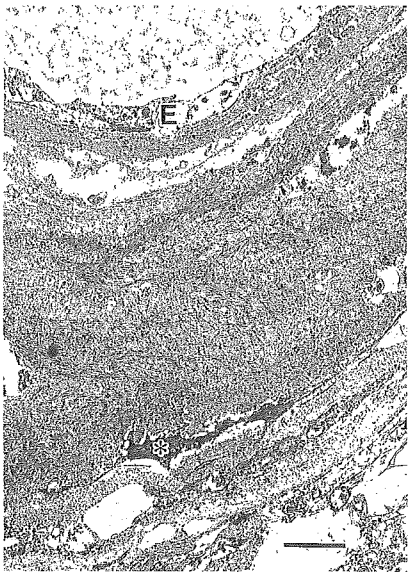

図2　CAAの皮質血管(電子顕微鏡像)
多量のアミロイド細線維が血管壁に蓄積し，中膜平滑筋細胞の変性(＊印)を伴っている．Eは内皮細胞を示す．×14,300，bar＝1 μm.

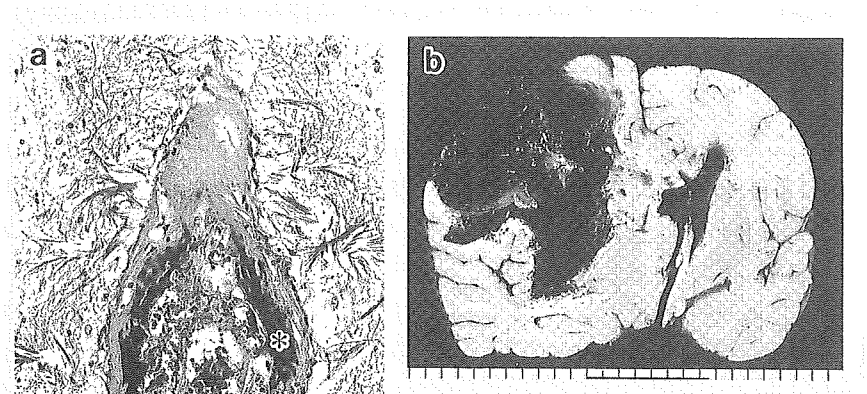

図3　CAAの随伴血管変化(a)及びCAA関連脳出血(b)
皮質小動脈は微小動脈瘤様拡張を示し，血管壁のフィブリノイド壊死(＊印)を伴っている(a)．この微小動脈瘤様病変はアミロイドが沈着している血管セグメントの中央部に生じ，出血の原因となり得る変化である(Maeda, et al. Stroke **24**：1857-1864, 1993)．CAAに関して右前頭―頭頂部に生じた大出血はくも膜下に穿破している(b)．a，Masson's trichrome染色，×170.

神経細胞特異的に過剰発現させたマウスがヒトのCAA同様の病変を示すことなどから，CAAのAβの由来は主には神経細胞である可能性が高い．神経細胞由来のAβは，毛細血管レベルで脳の間質液排出経路である血管周囲へと入り脳外へ排出されるが，この排出経路において血管壁に捕捉されることがCAAの発生機序として考えられている．高度のCAAは細動脈硬化と強く相関し，細動脈硬化による血管機能低下がAβの蓄積を促進している可能性があることが報告されている[8]．

ADの危険因子として確立されているApoEε4はCAAの程度と関連するが、一方，ADの防御因子と考えられているApoEε2は，CAA関連脳出血やその基盤となるCAA随伴血管変化と関連していることが欧米から報告されている．

5．CAAと痴呆及びADとの関連

高度のCAAを有する例では痴呆がしばしば認められる．高齢者CAAの痴呆の原因としては，CAAに関連する脳血管障害(多発・再発性の脳出血，白質脳症など)による脳血管性痴呆，ADの合併，両者の混合型などがあり，ADの亜型(vascular variant)と言うべき例も含まれる[14]．

AD病変(SP／NFT／神経細胞脱落)とCAAとの関連をは，多数の高齢者において脳全体ではSP／NFTとCAAは関連する[15]が，両者の脳内分布では相関がない[7)9)16]．CAAは血管周囲性SPの形成などの直接的な機序のみでなく，血管機能障害を介する間接的な機序でAD病変を加速させている可能性があり[17]，Aβ沈着血管の機能的側面については更なる検討が必要である．

ADにおけるCAA以外の血管病変及び血管性脳病変

1．微小血管病変及び細動脈硬化

形態学的研究及び生化学的研究により，ADではCAA以外に微小血管(毛細血管や細動脈)の変性が認められることが報告されている[18]．それには血管内皮や平滑筋細胞基底膜の変化などが含まれる[18]．こうした微小血管系の異常は，CAAとともに脳の局所灌流や酸素供給，血管壁におけるAβトランスポートの障害などを通じてAD病変に関与する可能性がある．

細動脈硬化はADにて対照群と比較して有意に高度に認められること[2)8)16)19]，細動脈硬化の進行度がNFTやSPの進行度と相関すること[15]，高血圧，糖尿病，高脂血症などの細動脈硬化を促進する因子がAD発症の危険因子でもあること[2]などが報告されている．これらは細動脈硬化がAD病変の発生や進行に影響を及ぼしている可能性を示唆

するが，その関与の程度やメカニズムの詳細は不明である．細動脈硬化に伴う血流量の低下による低酸素状態がタウ蛋白の異常なリン酸化を引き起こすとの報告がある[17]．

2．虚血性病変・大脳白質病変

虚血性病変(脳梗塞，皮質下ラクナ，海馬硬化，大脳白質病変)がADにて対照群と比較して有意に多数認められたとの報告があり[2)16)19)]，血管病変がADではしばしばみられるとの報告(前述)と関連する。これらの脳病変はそれ自体で痴呆を引き起こし得るため，ADにおける痴呆症状に影響を与えていることは間違いないが，AD病変との混在が見られる場合，それぞれがどの程度痴呆に関与しているかの判断〔"(ADと脳血管性痴呆の)混合型痴呆"や"血管性病変を伴うAD"など〕は必ずしも容易ではない．

ADでは脳病理所見や画像診断で大脳白質病変がよく見られる．大脳白質は虚血に対して非常に脆弱であるとされており，穿通枝が細動脈硬化やCAAに侵された場合に慢性的な低灌流に陥ることが一因であるが，ADでは大脳皮質に広範な神経細胞脱落を認めるため，それに伴う軸索の減少が白質病変に関与していることも考えられる．細動脈硬化は白質の髄鞘脱落とよく関連するが，CAAは白質病変との直接的な関連に乏しく[8)]，高度のCAAを有しながら白質病変がない例もあり，CAA関連白質脳症についてはCAA以外の因子(血圧の変化など)が加わることにより生じる可能性がある．

おわりに

ADにおける血管病変を病理学的側面より概説した．ADと血管病変，それに伴う血管性脳病変とのかかわりについてはいまだ不明な点も多いが，ADの病理発生や病態に影響を与え，痴呆症状に寄与していることは間違いない．今後，血管病変，あるいは血管病変をもたらす因子がどのようにAD病変の発生や進展に寄与し，症状を修飾するかを明らかにすることが必要であり，それはADの新しい予防・治療法の開発に繋がる．今後の研究の進展を期待したい．

文　献

1) Mirra SS, Hyman BT : Ageing and dementia. *in* Greenfield's neuropathology (7th ed), ed by Graham DI, London, Lantos PL, Arnold, 195-272,2002
2) Jellinger KA : Alzheimer disease and cerebrovascular pathology : an update. J Neural Transm **109** : 813-836, 2002
3) Yamada M : Cerebral amyloid angiopathy : an overview. Neuropathology **20** : 8-22, 2000
4) Itoh Y, Yamada M, Hayakawa M, et al : Cerebral amyloid angiopathy : a significant cause of cerebellar as well as lobar cerebral hemorrhage in the elderly. J Neurol Sci **116** : 135-141, 1993
5) Yamada M, Tsukagoshi H, Otomo E, et al : Cerebral amyloid angiopathy in the aged. J Neurol **234** : 371-376, 1987
6) Ellis RJ, Olichney JM, Thal LJ, et al : Cerebral amyloid angiopathy in the brains of patients with Alzheimer's disease : the CERAD experience, part XV. Neurology **46** : 1592-1596, 1996
7) Attems J, Jellinger KA : Only cerebral capillary amyloid angiopathy correlates with Alzheimer pathology—a pilot study. Acta Neuropathol (Berl) **107** : 83-90, 2004
8) Tian J, Shi J, Bailey K, et al : Relationships between arteriosclerosis, cerebral amyloid angiopathy and myelin loss from cerebral cortical white matter in Alzheimer's disease. Neuropathol Appl Neurobiol **30** : 46-56, 2004
9) 山田正仁：脳アミロイドアンギオパチー．神経内科 **58**(Suppl.3)：551-564, 2003
10) Revesz T, Ghiso J, Lashley T, et al : Cerebral amyloid angiopathies : a pathologic, biochemical, and genetic view. J Neuropathol Exp Neurol **62** : 885-898, 2003
11) Maeda A, Yamada M, Itoh Y, et al : Computer-assisted three-dimensional image analysis of cerebral amyloid angiopathy. Stroke **24** : 1857-1864, 1993
12) Weller RO, Nicoll JA : Cerebral amyloid angiopathy : Pathogenesis and effects on the ageing and Alzheimer brain. Neurol Res **25** : 611-616, 2003
13) Preston SD, Steart PV, Wilkinson A, et al : Capillary and arterial cerebral amyloid angiopathy in Alzheimer's disease : defining the perivascular route for the elimination of amyloid beta from the human brain. Neuropathol Appl Neurobiol **29** : 106-117, 2003
14) Yamada M, Itoh Y, Suematsu N, et al : Vascular variant of Alzheimer's disease characterized by severe plaque-like beta protein angiopathy. Dement Geriatr Cogn Disord **8** : 163-168, 1997
15) Thal DR, Ghebremedhin E, Orantes M, et al : Vascular pathology in Alzheimer disease : correlation of cerebral amyloid angiopathy and arteriosclerosis/lipohyalinosis with cognitive decline. J Neuropathol Exp Neurol **62** : 1287-1301, 2003
16) Tian J, Shi J, Bailey K, et al : Association between apolipoprotein E e4 allele and arteriosclerosis, cerebral amyloid angiopathy, and cerebral white matter damage in Alzheimer's disease. J Neurol Neurosurg Psychiatry **75** : 696-699, 2004
17) Grammas P, Yamada M, Zlokovic B : The cerebromicrovasculature : a key player in the pathogenesis of Alzheimer's disease. J Alzheimers Dis **4** : 217-223, 2002
18) Kalaria RN : Small vessel disease and Alzheimer's dementia : pathological considerations. Cerebrovasc Dis **13** (Suppl. 2) : 48-52, 2002
19) Jellinger KA, Mitter-Ferstl E : The impact of cerebrovascular lesions in Alzheimer disease—a comparative autopsy study. J Neurol **250** : 1050-1055, 2003